Toward a Retail Market for Distribution Grids

Rabab Haider, *Graduate Student Member, IEEE*, Stefanos Baros, *Member, IEEE*, Yasuaki Wasa, *Member, IEEE*, Jordan Romvary, *Member, IEEE*, Kenko Uchida, *Member, IEEE*, and Anuradha M. Annaswamy, *Fellow, IEEE*

***Abstract*—Modern active distribution grids are characterized by the increasing penetration of distributed energy resources (DERs). Proper coordination and scheduling of these DERs requires a local retail market which can operate at the distribution grid level. In this paper, we propose a retail market for optimally managing and scheduling DERs, and coordinating ancillary services in a distribution grid. Our proposed retail market leverages a recently proposed distributed proximal atomic coordination (PAC) algorithm which has several advantages over other distributed algorithms, with reduced local computational effort and enhanced privacy. We describe how the market can be implemented using a Distribution System Operator (DSO), whose representatives are located at the primary feeder level and workers are located at the substation level, and how the DSO will interact with the Wholesale Electricity Market. Finally, we extensively validate the performance of the proposed retail market via simulations of three networks: a real distribution grid in Tokyo, a balanced IEEE 123-bus distribution grid, and a modified IEEE 13-bus network. Our results show that the proposed market is practical and can be easily implemented in distribution grids, resulting in optimal real-time scheduling of DERs and compensation in the form of distributed locational marginal prices.**

***Index Terms*—Distribution grid market, optimal power flow, distributed algorithm, ancillary market.**

NOMENCLATURE

$P^{\mathrm{G}}_{\mathbf{j}}, Q^{\mathrm{G}}_{\mathbf{j}}$	Real and reactive power generation at bus $\mathbf{j}$.
$P^{\mathrm{L}}_{\mathbf{j}}, Q^{\mathrm{L}}_{\mathbf{j}}$	Real and reactive power consumption at bus $\mathbf{j}$.
$v_{\mathbf{j}}$	Squared magnitude of local voltage level all at bus $\mathbf{j}$; $v_{\mathbf{j}} = \lvert\hat{V}_j\rvert^2$.
$P_{\mathbf{i},\mathbf{j}}, Q_{\mathbf{i},\mathbf{j}}$	Real and reactive power flow in branch $(\mathbf{i},\mathbf{j})$;
$l_{\mathbf{i},\mathbf{j}}$	Squared magnitude of current flow along the $(\mathbf{i},\mathbf{j})$-branch; $l_{\mathbf{i},\mathbf{j}} = \lvert\hat{I}_{i,j}\rvert^2$.
$R_{\mathbf{i},\mathbf{j}}, X_{\mathbf{i},\mathbf{j}}$	Resistance and reactance of the $(\mathbf{i},\mathbf{j})$-branch.
$\tilde{v}^{[\mathbf{j}]}_{\mathbf{i}}$	Local $\mathbf{j}$-th atomic copy of the upstream voltage phasor magnitude.
$\tilde{P}^{[\mathbf{j}]}_{\mathbf{j},\mathbf{h}}, \tilde{Q}^{[\mathbf{j}]}_{\mathbf{j},\mathbf{h}}$	Local $\mathbf{j}$-th atomic copies of the downstream real and reactive power flows.
$\underline{(\cdot)}$	Lower limits on local bus variables (ex. $\underline{P}^{\mathrm{G}}_{\mathbf{j}}$).
$\overline{(\cdot)}$	Upper limits on local bus variables (ex. $\overline{P}^{\mathrm{G}}_{\mathbf{j}}$).
$\overline{S^2_{\mathbf{i},\mathbf{j}}}$	Thermal limit of the total apparent power allowed on the $(\mathbf{i},\mathbf{j})$-branch.
$P^{\mathrm{L0}}_{\mathbf{j}}, Q^{\mathrm{L0}}_{\mathbf{j}}$	Baseline real and reactive power consumption of flexible consumers.
$\mathbf{y}$	Decision vector for network, which is a collection of the subvectors $\mathbf{y}_{\mathbf{j}}$ that capture the variables of each bus $\mathbf{j}$; $\mathbf{y} = [\mathbf{P}^{\mathrm{G}}; \mathbf{P}^{\mathrm{L}}; \mathbf{Q}^{\mathrm{G}}; \mathbf{Q}^{\mathrm{L}}; \mathbf{v}; \mathbf{l}; \mathbf{P}; \mathbf{Q}]$. Bold characters here denote vectors.
$\mathbf{a}_{\mathbf{j}}$	Atomic version of the subvector $\mathbf{y}_{\mathbf{j}}$, also containing local copies of the coupling variables.
$\boldsymbol{\mu}_{\mathbf{j}}$	Lagrange multipliers corresponding to the voltage bus equality, real power balance equality, and reactive power balance equality constraints: $[\mu^{\mathrm{v}}_{\mathbf{j}} \;\; \mu^{\mathrm{P}}_{\mathbf{j}} \;\; \mu^{\mathrm{Q}}_{\mathbf{j}}]$
$\beta^{\mathrm{PG}}_{\mathbf{j}}, \beta^{\mathrm{QG}}_{\mathbf{j}}$	Cost coefficients of the generation cost.
$\beta^{\mathrm{PL}}_{\mathbf{j}}, \beta^{\mathrm{QL}}_{\mathbf{j}}$	Cost coefficients of the load utility functions.
$\lambda^{\mathrm{P}}_{\mathbf{l}}, \lambda^{\mathrm{Q}}_{\mathbf{l}}$	Locational marginal prices (LMPs) corresponding to the distribution grid feeder.
$\lambda^{\mathrm{P}}_{\mathrm{retail}}, \lambda^{\mathrm{Q}}_{\mathrm{retail}}$	Retail electricity prices, assumed constant
ξ	Parameter capturing the tradeoff between local bus generation costs and global branch losses.
$\mathcal{S}$	Set of all substations in a distribution grid.
$\mathcal{F}_s$	Set of all feeders per substation s.
$\mathcal{B}$	Set of buses connected to (and including) feeder l at bus $j^{\#}$.
$\mathcal{T}_{\mathrm{D}} \subseteq \mathcal{B} \times \mathcal{B}$	All grid distribution lines.

Manuscript received February 4, 2019; revised June 21, 2019 and November 6, 2019; accepted April 24, 2020. Date of publication May 21, 2020; date of current version October 21, 2020. This work was supported in part by NSF under Award EFRI-1441301, in part by the Department of Energy, Office of International Affairs and Office of Electricity under Award DE-IA0000025, in part by JST CREST under Grant JPMJCR15K2, and in part by the Siemens Corporate Technology, Princeton, NJ, USA. Paper no. TSG-00187-2019. *(Corresponding author: Rabab Haider.)*

Rabab Haider, Stefanos Baros, Jordan Romvary, and Anuradha M. Annaswamy are with the Department of Mechanical Engineering, Massachusetts Institute of Technology, Cambridge, MA 02139 USA (e-mail: rhaider@mit.edu; sbaros@mit.edu; jromvary@mit.edu; aanna@mit.edu).

Yasuaki Wasa and Kenko Uchida are with the Department of Electrical Engineering and Bioscience, Waseda University, Tokyo 169-8555, Japan (e-mail: wasa@aoni.waseda.jp; kuchida@waseda.jp).

Color versions of one or more of the figures in this article are available online at http://ieeexplore.ieee.org.

Digital Object Identifier 10.1109/TSG.2020.2996565

I. INTRODUCTION

ONE OF the central features of the emerging Smart Grid is a highly transformed distribution grid with a high penetration of distributed energy resources (DERs). These DERs include distributed generation (DG), demand response (DR) compatible loads, and storage devices such as batteries and electric vehicles. As these DERs can be owned and operated

by different stake holders, the efficient and reliable operation of the distribution grid requires an overall market structure that allows the procurement and integration of power generation from these DERs, while maintaining data privacy.

The current practice in the United States for the integration of DGs is for them to participate in the Wholesale Electricity Market (WEM) [1]. While this participation largely pertains to DGs, certain amount of participation also occurs from DR units and storage devices [2], as evidenced by FERC order 841. Despite these recent advances, as the number of DERs grows and renewable generation continues to increase, particularly small-scale DERs in the distribution grid, the WEM alone may not suffice in realizing efficient and reliable power delivery. Thus, a retail market that oversees the participation of DERs in the distribution grid and implements a suitable mechanism for their scheduling and compensation is highly necessary.

The need for such a market has gained considerable traction, with various approaches being taken. The concept of transactive energy is one such promising design, whereby a service-based value of power is used to influence desirable behaviors from various autonomous agents, which include prosumers and DERs at the grid's edge, at fast timescales [3], [4]. In this way, transactive energy is providing a link between the physical power flow in the grid, and market derivatives and regulatory constructs. In this framework, an independent agent does not have to cede control of its DERs to a centralized authority; rather it reacts to price signals to provide services to the grid, for which it will be compensated.

As the number of DERs and prosumers increases, more structure is warranted to coordinate and carry out the underlying transactive energy schemes. New operational entities such as a Distributed System Operator (DSO) and a retail market coordinated by DSOs may be needed. The DSO can take on various roles, including maintaining system reliability, facilitating transactions between agents and aggregators, and acting in the capacity of a utility whereby the DSO procures energy and coordinates a retail market [5]. The latter is the focus of this paper, in which we propose a structured set of market interactions for the distribution grid, each one of which may be viewed as a transactive energy scheme. The retail market consists of an energy market and ancillary services market, both coordinated by a DSO. The energy market leverages a recently developed distributed optimization algorithm [6], [7], with its solution serving as the schedule and retail prices for DERs. The ancillary market is based on a simple optimization based algorithm. In both markets, DERs are compensated based on the need for their specific service.

The coordination of power delivery as well as the overall market design as the number of DERs begins to increase are areas of active research [8]–[34]. The literature herein can be broadly grouped into centralized [11]–[17], decentralized [18]–[23], and distributed approaches [24]–[34], with this paper being a member of the third category. Reference [10] is a survey paper that gives an excellent overview of different market approaches to integrating DERs, particularly focusing on prosumers and flexible loads.

References [11]–[17] consist of centralized market perspectives. A hierarchical market structure is proposed in [11] and [12] to interlace the operation of the WEM with the retail market, where a Distributed Network Operator (DNO) is responsible for operating the market and load aggregators for smooth interactions with the WEM. In [13] the optimal dispatch of DR units in a distribution grid occurs through collective participation in the WEM, while in [14], competitive participation for the provision of ancillary services is used. The authors in [15] propose a centralized market where the DSO schedules the day-ahead transactions for DERs in the distribution grid. Bids are made by prosumers, generators, and microgrids, and both the DSO market and WEM are simulated iteratively until both wholesale price and distribution-level Locational Marginal Prices (d-LMP) are determined. The DSO is assumed to maximize their payoff. In this design, DC power flow is used, which can yield large errors for the highly unbalanced distribution grids. Meanwhile, [16] and [17] use an iterative procedure to solve the Optimal Power Flow (OPF) problem based on a Three-Phase Current Injection Method (TCIM), and determine d-LMPs per phase per bus through difference of power constraints. Due to the centralized perspective proposed in these papers, agents are required to disclose operating constraints and utility functions to a central entity. In doing so, the agents lose data privacy; additionally, in market designs where the DSO is maximizing its own profit, this acts against the best interest of the market players. In addition, such a calculation of d-LMPs for a distribution grid is computationally significantly harder than the typically smaller sized transmission grid, and the central optimization problem can quickly become intractable with large number of DERs participating. Finally, these papers focus largely on d-LMP calculation, rather than proposing holistic market interactions.

An attractive alternative to centralized perspectives is a decentralized one. Herein, each agent is assumed to use local information to make decisions, but is otherwise unaware of the presence of others and do not therefore communicate with them. Such decentralized EMS are proposed in [18] and [19], to coordinate the operation of DERs and networked microgrids in the distribution grid. Decentralized market designs have also been proposed in [20]–[23]. The authors of [20] introduce a decentralized market with bilateral trading rules which result in fair allocation of the line losses. However, the relation between trading rules and optimal dispatch of DERs are not addressed. More recent works are those in [21]–[23], each of which consist of different approaches. The market in [21] is a peer-to-peer (P2P) structure in which different agents bid in the marketplace to determine day-ahead energy schedules. The market in [22] uses blockchain to facilitate energy transactions, while [23] makes use of game-theoretic approaches to determine real-time d-LMPs. All of these proposed markets have either limited interactions or do not accommodate interactions with the WEM. The main disadvantage of decentralized solutions simply stems from the fact that each agent's decision is local and therefore predicated on the assumption that coupling with others is weak. This leads to limited applicability without intervention from a centralized decision maker and therefore cannot be scaled up, especially as the number of DERs increases.

This brings us to the third category, of distributed solutions, where the agents communicate with peers/neighbours to achieve a common objective, thus potentially leading to an optimal global objective being achieved. Since distributed methods rely primarily on local computations at each node and P2P exchange of information, they are computationally tractable. Moreover, if well designed, they can be resilient to communication link and single-point failures, and can preserve the private information of the DERs, while still realizing network-level objectives. Papers [24]–[28] correspond to this category. The work in [24] introduces an algorithm with a parallel architecture that can concurrently yield price discovery along with optimal scheduling of resources in both transmission and distribution grids. Although the problem formulation is very detailed, the proposed algorithm is quite complex and thus practical implementation is challenging. In [25], a day-ahead energy market is run by a DNO, using the predictor corrector proximal multiplier method. The DNO maximizes its profits while determining a retail price for the DERs. In the proposed structure, all agents share the same retail price, leading to inefficient pricing; since agents are providing different grid services, they should be compensated based on the need for their specific flexibility during the scheduled period. Many papers such as [26]–[28] use consensus based approaches. In [26], a consensus-based algorithm is used to discover electricity prices, when neglecting network constraints and congestion limits. In [27], a cooperative energy management algorithm is designed, whereby local prices and generator set points are determined; however, generators must share marginal costs with neighbours in order to determine the global price of energy, reducing privacy in the network. Further, the interpretation of this global price is unclear. Finally, consensus+innovations approaches are used in [28] to address state estimation, economic dispatch, and OPF problems. To utilize the consensus+innovations approach for economic dispatch, the marginal costs at each bus are required to be the same at optimality. This assumption is relaxed for the OPF problem, however only for congested networks. Further, agents are still required to share their marginal costs with neighbours. A discussion on the overall structure of the market and interactions with the WEM are also lacking in these works. For the most part, consensus based approaches do not preserve privacy of constraints and/or prices, reducing applicability for market applications, where even marginal prices should be kept private. It should be noted that distributed approaches have also been employed for general EMS applications (see for example [29]–[34]). By in large, EMS systems focus on the operational aspects of the grid, and deal with system monitoring and control, generation and dispatch set points, and energy scheduling. These functions are not concerned with market derivatives for services provided to the grid by DERs. As our focus is on a market design with DERs, a discussion of these papers is beyond the scope and is therefore omitted.

In contrast to previous works, the focus of this paper is to develop a comprehensive retail market with appropriate pricing for DERs in a distribution grid. For this purpose, we utilize a distributed architecture which maintains complete privacy for DERs. In addition to price discovery, the framework provides guidelines for coupling connected distribution grids, and interactions with the WEM. The proposed retail market is structured around a recently developed distributed optimization algorithm, the proximal atomic coordination algorithm (PAC) [6], [7]. The following are the specific contributions of the paper.

- We propose a novel retail market mechanism for distribution grids under high penetration of DERs, where decisions are carried out by a DSO. The DSO oversees two markets: (1) an energy market for DER scheduling and real-time market settlements (d-LMP) through bilateral contracts; and (2) an ancillary market which oversees transactions for alert conditions between primary feeders in the distribution network. The DSO acts like a proactive utility, in that it accepts the LMP as traditionally determined by the WEM, but optimally uses DERs within the distribution network, and only requests service from the WEM for net loads beyond its DER capabilities.
- We numerically verify and extensively validate the proposed retail market via simulations of a real distribution grid in Tokyo, Japan, and the IEEE 123-bus distribution grid representative of the US, both over a period of 24 hours. We also validate the performance of the ancillary services algorithm on a 3 feeder network comprised of modified IEEE 13-bus networks. We also illustrate how the market interactions will take place and compute the settlements under the studied scenarios. Our results show potential savings for the DSO under this new market mechanism.

The rest of the paper is organized as follows. Section II briefly presents the distributed PAC algorithm, and the formulation of the OPF problem for distribution grids. Section III introduces the structure of the retail market and interactions between different market players, and describes the DSO revenue metric used in Section IV for performance evaluation of the proposed retail market via numerical simulations. Conclusions are provided in Section V.

II. A Distributed PAC Algorithm

The retail market oversees the scheduling for DERs and the retail price, termed a d-LMP, as determined by the Optimal Power Flow (OPF) problem. The OPF determines power injections and voltages at each bus ($P^{\mathrm{G}}_{\mathbf{j}}, P^{\mathrm{L}}_{\mathbf{j}}, Q^{\mathrm{G}}_{\mathbf{j}}, P^{\mathrm{L}}_{\mathbf{j}}$ and $v_{\mathbf{j}}$) and flow variables in the i-jth branch ($P_{\mathbf{i},\mathbf{j}}, Q_{\mathbf{i},\mathbf{j}}, l_{\mathbf{i},\mathbf{j}}$) as its decisions, while minimizing the total expenditure (payments to generating units less revenue from consumption units) and power losses. Storage is not considered in this paper. We consider grids with radial topology which are represented as a directed graph $\mathbf{\Gamma}_{\mathrm{D}} = \langle \mathcal{B}, \mathcal{T}_{\mathrm{D}} \rangle$, with $\mathcal{B}$ the graph vertices and $\mathcal{T}_{\mathrm{D}}$ the directed edges.

A. Statement of OPF Problem

This problem is formally stated as:

$$\min_{\mathbf{y}\in\mathbb{R}^{|\mathbf{y}|}} \; f^{\mathrm{OPF}}(\mathbf{y})$$

$$\text{subject to: } \underline{P^{\mathrm{G}}_{\mathbf{j}}} \le P^{\mathrm{G}}_{\mathbf{j}} \le \overline{P^{\mathrm{G}}_{\mathbf{j}}}, \qquad \forall \mathbf{j} \in \mathcal{B}$$

$$
\begin{aligned}
&\underline{P^{\mathrm{L}}_{\mathbf{j}}} \le P^{\mathrm{L}}_{\mathbf{j}} \le \overline{P^{\mathrm{L}}_{\mathbf{j}}}, && \forall \mathbf{j} \in \mathcal{B}\\
&\underline{Q^{\mathrm{G}}_{\mathbf{j}}} \le Q^{\mathrm{G}}_{\mathbf{j}} \le \overline{Q^{\mathrm{G}}_{\mathbf{j}}}, && \forall \mathbf{j} \in \mathcal{B}\\
&\underline{Q^{\mathrm{L}}_{\mathbf{j}}} \le Q^{\mathrm{L}}_{\mathbf{j}} \le \overline{Q^{\mathrm{L}}_{\mathbf{j}}}, && \forall \mathbf{j} \in \mathcal{B}\\
&\underline{v_{\mathbf{j}}} \le v_{\mathbf{j}} \le \overline{v_{\mathbf{j}}}, && \forall \mathbf{j} \in \mathcal{B}\\
&P^2_{\mathbf{i},\mathbf{j}} + Q^2_{\mathbf{i},\mathbf{j}} \le \overline{S}^2_{\mathbf{i},\mathbf{j}}, && \forall (\mathbf{i},\mathbf{j}) \in \mathcal{T}_{\mathrm{D}}\\
&P^2_{\mathbf{i},\mathbf{j}} + Q^2_{\mathbf{i},\mathbf{j}} \le v_{\mathbf{i}} l_{\mathbf{i},\mathbf{j}}, && \forall (\mathbf{i},\mathbf{j}) \in \mathcal{T}_{\mathrm{D}}\\
&0 \le l_{\mathbf{i},\mathbf{j}} \le \overline{S}^2_{\mathbf{i},\mathbf{j}}/\overline{v}_{\mathbf{i}}, && \forall (\mathbf{i},\mathbf{j}) \in \mathcal{T}_{\mathrm{D}}\\
&v_{\mathbf{j}} = v_{\mathbf{i}} - 2\big(R_{\mathbf{i},\mathbf{j}} P_{\mathbf{i},\mathbf{j}} + X_{\mathbf{i},\mathbf{j}} Q_{\mathbf{i},\mathbf{j}}\big) + \Big(R^2_{\mathbf{i},\mathbf{j}} + X^2_{\mathbf{i},\mathbf{j}}\Big) l_{\mathbf{i},\mathbf{j}}, && \forall (\mathbf{i},\mathbf{j}) \in \mathcal{T}_{\mathrm{D}}\\
&P^{\mathrm{G}}_{\mathbf{j}} - P^{\mathrm{L}}_{\mathbf{j}} = -P_{\mathbf{i},\mathbf{j}} + R_{\mathbf{i},\mathbf{j}} l_{\mathbf{i},\mathbf{j}} + \sum_{\mathbf{k}:(\mathbf{j},\mathbf{k})\in\mathcal{T}} P_{\mathbf{j},\mathbf{k}}, && \forall (\mathbf{i},\mathbf{j}) \in \mathcal{T}_{\mathrm{D}}\\
&Q^{\mathrm{G}}_{\mathbf{j}} - Q^{\mathrm{L}}_{\mathbf{j}} = -Q_{\mathbf{i},\mathbf{j}} + X_{\mathbf{i},\mathbf{j}} l_{\mathbf{i},\mathbf{j}} + \sum_{\mathbf{k}:(\mathbf{j},\mathbf{k})\in\mathcal{T}} Q_{\mathbf{j},\mathbf{k}}, && \forall (\mathbf{i},\mathbf{j}) \in \mathcal{T}_{\mathrm{D}}\\
&P^{\mathrm{G}}_{\mathbf{i}} - P^{\mathrm{L}}_{\mathbf{i}} = \sum_{\mathbf{k}:(\mathbf{i},\mathbf{k})\in\mathcal{T}} P_{\mathbf{i},\mathbf{k}}, && \forall \mathbf{i} \in \mathcal{F}\\
&Q^{\mathrm{G}}_{\mathbf{i}} - Q^{\mathrm{L}}_{\mathbf{i}} = \sum_{\mathbf{k}:(\mathbf{i},\mathbf{k})\in\mathcal{T}} Q_{\mathbf{i},\mathbf{k}}, && \forall \mathbf{i} \in \mathcal{F}
\end{aligned} \tag{1}
$$

where the cost function is defined as:

$$
f^{\text{G-Cost}}_{\mathbf{j}}(\mathbf{y}) = \begin{cases} \beta^{\mathrm{PG}}_{\mathbf{j}}\Big(P^{\mathrm{G}}_{\mathbf{j}}\Big)^2 + \beta^{\mathrm{QG}}_{\mathbf{j}}\Big(Q^{\mathrm{G}}_{\mathbf{j}}\Big)^2, & \text{if } \mathbf{j} \in \tilde{\mathcal{B}} \triangleq \mathcal{B} \setminus \mathcal{F} \\ \lambda^{\mathrm{P}}_{\mathbf{j}} P^{\mathrm{G}}_{\mathbf{j}} + \lambda^{\mathrm{Q}}_{\mathbf{j}} Q^{\mathrm{G}}_{\mathbf{j}}, & \text{if } \mathbf{j} \in \mathcal{F} \end{cases} \tag{2}
$$

$$
f^{\text{L-Util}}_{\mathbf{j}}(\mathbf{y}) = \begin{cases} -\beta^{\mathrm{PL}}_{\mathbf{j}}\Big(P^{\mathrm{L}}_{\mathbf{j}} - P^{\mathrm{L0}}_{\mathbf{j}}\Big)^2 - \beta^{\mathrm{QL}}_{\mathbf{j}}\Big(Q_{\mathbf{j}} - Q^{\mathrm{L0}}_{\mathbf{j}}\Big)^2, & \text{if } \mathbf{j} \in \tilde{\mathcal{B}} \\ 0, & \text{if } \mathbf{j} \in \mathcal{F} \end{cases} \tag{3}
$$

$$
f^{\mathrm{Loss}}_{\mathbf{i},\mathbf{j}}(\mathbf{y}) = R_{\mathbf{i},\mathbf{j}} l_{\mathbf{i},\mathbf{j}}, \quad \text{if}(\mathbf{i},\mathbf{j}) \in \mathcal{T} \tag{4}
$$

$$
f^{\mathrm{OPF}}(\mathbf{y}) = \sum_{\mathbf{j}\in\mathcal{B}} \Big[f^{\text{G-Cost}}_{\mathbf{j}}(\mathbf{y}) - f^{\text{L-Util}}_{\mathbf{j}}(\mathbf{y}) \Big] + \xi \left[\sum_{(\mathbf{i},\mathbf{j})\in\mathcal{T}} f^{\mathrm{Loss}}_{\mathbf{i},\mathbf{j}}(\mathbf{y}) \right]. \tag{5}
$$

Here, $f^{\text{G-Cost}}_{\mathbf{j}}$ corresponds to the generation cost function of distributed generators, $f^{\text{L-Util}}_{\mathbf{j}}$ to the disutility function of the flexible consumers capturing their dissatisfaction for curtailing their consumption, $f^{\mathrm{Loss}}_{\mathbf{i},\mathbf{j}}$ to the power losses cost function where losses are due to the line resistances, and f^{OPF} to the aggregate cost function of the OPF problem.

The compositions of the subvectors $\mathbf{y}_{\mathbf{j}}$ are different depending upon the type of bus. In particular, if $(\mathbf{i},\ \mathbf{j}), \{(\mathbf{j}, \mathbf{h}_{\mathbf{j}})\}_{\mathbf{j}\in[n]} \in \mathcal{T}_{\mathrm{D}}$, the vector $\mathbf{y}_{\mathbf{j}}$ would be:

$$
\mathbf{y}_{\mathbf{j}} = \Big[P^{\mathrm{G}}_{\mathbf{j}};\, P^{\mathrm{L}}_{\mathbf{j}};\, Q^{\mathrm{G}}_{\mathbf{j}};\, Q^{\mathrm{L}}_{\mathbf{j}};\, v_{\mathbf{j}};\, v_{\mathbf{i}};\, P_{\mathbf{i},\mathbf{j}};\, Q_{\mathbf{i},\mathbf{j}};\, l_{\mathbf{i},\mathbf{j}};\, \big\{P_{\mathbf{j};\mathbf{h}_{\mathbf{j}}};\, Q_{\mathbf{j},\mathbf{h}_{\mathbf{j}}}\big\}_{\mathbf{j}\in[n]} \Big]
$$

If only $(\mathbf{i},\mathbf{j}) \in \mathcal{T}_{\mathrm{D}}$ (end node) by:

$$
\mathbf{y}_{\mathbf{j}} = \Big[P^{\mathrm{G}}_{\mathbf{j}};\, P^{\mathrm{L}}_{\mathbf{j}};\, Q^{\mathrm{G}}_{\mathbf{j}};\, Q^{\mathrm{L}}_{\mathbf{j}};\, v_{\mathbf{j}};\, v_{\mathbf{i}};\, P_{\mathbf{i},\mathbf{j}};\, Q_{\mathbf{i},\mathbf{j}};\, l_{\mathbf{i},\mathbf{j}} \Big]
$$

If only $\{(\mathbf{j}, \mathbf{h}_{\mathbf{j}})\}_{\mathbf{j}\in[n]} \in \mathcal{T}_D$ (feeder node) by:

$$
\mathbf{y}_{\mathbf{j}} = \Big[P^{\mathrm{G}}_{\mathbf{j}};\, P^{\mathrm{L}}_{\mathbf{j}};\, Q^{\mathrm{G}}_{\mathbf{j}};\, Q^{\mathrm{L}}_{\mathbf{j}};\, v_{\mathbf{j}};\, \big\{P_{\mathbf{j};\mathbf{h}_{\mathbf{j}}};\, Q_{\mathbf{j},\mathbf{h}_{\mathbf{j}}}\big\}_{\mathbf{j}\in[n]} \Big]
$$

where $\mathbf{h}_{\mathbf{j}}$ denotes the set of downstream buses connected to bus $\mathbf{j}$. With the vectors defined above, we compactly state the optimization problem (1) as:

$$
\begin{aligned}
\min_{\mathbf{y}} \ & \sum_{\mathbf{j}\in\mathcal{B}} f^{\mathrm{OPF}}_{\mathbf{j}}(\mathbf{y}_{\mathbf{j}}) \\
\text{subject to: } & g_{\mathbf{j}}(\mathbf{y}_{\mathbf{j}}) \le \mathbf{0}, \quad \mathbf{j} \in \mathcal{B} \\
& \tilde{\mathbf{G}}_{\mathbf{j}} \mathbf{y}_{\mathbf{j}} = \mathbf{0}, \quad \mathbf{j} \in \mathcal{B}
\end{aligned} \tag{6}
$$

where $g_{\mathbf{j}}$ represents the local bus and branch inequality constraints and $\tilde{\mathbf{G}}_{\mathbf{j}}$ the branch equality constraints. We note that the convex relaxation in [35] has been employed in the voltage inequality of Problem 1.

B. Atomization of the OPF Problem

The solution to the *relaxed OPF problem* (6), rOPF, will be attained in a fully distributed fashion using the proximal atomic coordination (PAC) algorithm [6], [7]. In its current formulation, the rOPF problem (6) with local vectors $\mathbf{y}_{\mathbf{j}}$ is not fully decomposable into atoms, as the coupling variables $v_{\mathbf{i}}$, $P_{\mathbf{i},\mathbf{j}}$ and $Q_{\mathbf{i},\mathbf{j}}$, appear in both the $\mathbf{y}_{\mathbf{j}}$ and $\mathbf{y}_{\mathbf{i}}$ of two neighboring buses $\mathbf{j}$ and $\mathbf{i}$. To render the problem decomposable, we follow the required decomposition profile from [6], [7], and use local copies instead of the actual coupling variables in each $\mathbf{y}_{\mathbf{j}}$. Additional equality constraints are introduced to enforce these copies to coincide with the coupling variables at convergence. The resulting *atomized standard optimization relaxed OPF* (asorOPF) can then be solved in a fully distributed fashion. Atomizing each bus' variables, yields the asorOPF problem:

$$
\begin{aligned}
\min_{\mathbf{a}\in\mathbb{R}^{|\mathbf{a}|}} \ & \hat{f}^{\mathrm{OPF}}(\mathbf{a}) \\
\text{subject to: } & \text{Constraints from (1)}, && \forall \mathbf{j} \in \mathcal{B}, \\
& \forall (\mathbf{i},\mathbf{j}) \in \mathcal{T}, && \forall \mathbf{i} \in \mathcal{F} \\
& \tilde{v}^{[\mathbf{j}]}_{\mathbf{i}} - v_{\mathbf{i}} = 0, && \forall \mathbf{i} \in \mathcal{B} \\
& \tilde{P}^{[\mathbf{j}]}_{\mathbf{j},\mathbf{h}} - P_{\mathbf{j},\mathbf{h}} = 0, && \forall (\mathbf{j},\mathbf{h}) \in \mathcal{T} \\
& \tilde{Q}^{[\mathbf{j}]}_{\mathbf{j},\mathbf{h}} - Q_{\mathbf{j},\mathbf{h}} = 0, && \forall (\mathbf{j},\mathbf{h}) \in \mathcal{T}
\end{aligned} \tag{7}
$$

In general, we assume that bus $\mathbf{i}$ is closer than bus $\mathbf{j}$ to the feeder in a given branch $(\mathbf{i},\mathbf{j})$. Note that (7) differs from the original rOPF (1) only in the last three equalities, which enforce all local copies of the vector $\mathbf{y}_{\mathbf{j}}$ to coincide with the actual variables that are in $\mathbf{y}_{\mathbf{i}}$. We can compactly express these constraints in matrix form as:

$$
\mathbf{A}\mathbf{a} = \mathbf{0}, \tag{8}
$$

where $\mathbf{A}$ represents the adjacency matrix of Γ_{D}. Using (8) and augmenting $\hat{f}^{\mathrm{OPF}}(\mathbf{a}) \triangleq \sum_{\mathbf{j}\in\mathcal{B}} \hat{f}_{\mathbf{j}}(\mathbf{a}_{\mathbf{j}})$ using an indicator function, one can state the equivalent of (1) atomic formulation asorOPF problem compactly as:

$$
\begin{aligned}
\min_{\mathbf{a}\in\mathbb{R}^{|\mathbf{a}|}} \ & \sum_{\mathbf{j}\in\mathcal{B}} \hat{f}_{\mathbf{j}}(\mathbf{a}_{\mathbf{j}}) \\
\text{subject to: } & \tilde{\mathbf{G}}_{\mathbf{j}} \mathbf{a}_{\mathbf{j}} = \mathbf{0}, \quad \mathbf{j} \in \mathcal{B} \\
& \mathbf{A}_{\mathbf{j},-} \mathbf{a} = \mathbf{0}, \quad \mathbf{j} \in \mathcal{B}
\end{aligned} \tag{9}
$$

where $\mathbf{A}_{\mathbf{j},-}$ represents the rows of $\mathbf{A}$ that correspond to the coupling variables along $(\mathbf{i},\mathbf{j}) \in \mathcal{T}_{\mathrm{D}}$. The equality $\tilde{\mathbf{G}}_{\mathbf{j}}\mathbf{a}_{\mathbf{j}} = \mathbf{0}$ enforces Kirchhoff's Voltage Law and power balance constraints.

C. Distributed PAC Algorithm

Below is the PAC algorithm to solve (9) (see Appendix A and [6], [7] for details), which is based on a distributed linearized variant of the proximal method of multipliers [36], [37]:

$$\mathbf{a}_{\mathbf{j}}[\tau+1] = \mathbf{argmin}_{\mathbf{a}_{\mathbf{j}}}\left\{\tilde{\mathcal{L}}_{\rho,\gamma}\left(\mathbf{a}_{\mathbf{j}}, \tilde{\boldsymbol{\mu}}_{\mathbf{j}}[\tau], \tilde{\boldsymbol{\nu}}[\tau]; \mathbf{a}_{\mathbf{j}}[\tau]\right)\right\} \quad (10)$$

$$\boldsymbol{\mu}_{\mathbf{j}}[\tau+1] = \boldsymbol{\mu}_{\mathbf{j}}[\tau] + \rho\gamma_{\mathbf{j}}\tilde{\mathbf{G}}_{\mathbf{j}}\mathbf{a}_{\mathbf{j}}[\tau+1] \quad (11)$$

$$\tilde{\boldsymbol{\mu}}_{\mathbf{j}}[\tau+1] = \boldsymbol{\mu}_{\mathbf{j}}[\tau+1] + \rho\hat{\gamma}_{\mathbf{j}}\tilde{\mathbf{G}}_{\mathbf{j}}\mathbf{a}_{\mathbf{j}}[\tau+1] \quad (12)$$

$$\text{Communicate } \left\{\mathbf{a}_{\mathbf{j}}\right\}_{\mathbf{j}\in\mathcal{B}} \text{ according to } \boldsymbol{\Gamma}_{\mathbf{D}} \quad (13)$$

$$\boldsymbol{\nu}_{\mathbf{j}}[\tau+1] = \boldsymbol{\nu}_{\mathbf{j}}[\tau] + \rho\gamma_{\mathbf{j}}\mathbf{A}_{\mathbf{j},-}\mathbf{a}[\tau+1] \quad (14)$$

$$\tilde{\boldsymbol{\nu}}_{\mathbf{j}}[\tau+1] = \boldsymbol{\nu}_{\mathbf{j}}[\tau+1] + \rho\hat{\gamma}_{\mathbf{j}}\mathbf{A}_{\mathbf{j},-}\mathbf{a}[\tau+1]. \quad (15)$$

$$\text{Communicate } \left\{\tilde{\boldsymbol{\nu}}_{\mathbf{j}}\right\}_{\mathbf{j}\in\mathcal{B}} \text{ according to } \boldsymbol{\Gamma}_{\mathbf{D}} \quad (16)$$

In the above, $\rho > 0$ is the step-size and $\gamma_{\mathbf{j}}, \hat{\gamma}_{\mathbf{j}} > 0$ are two over-relaxation terms with $\gamma_{\mathbf{j}} > \hat{\gamma}_{\mathbf{j}}$. As shown in [6], [7] and Appendix B, the primal variables $\mathbf{a}$, and dual variables $\boldsymbol{\mu}$ and $\boldsymbol{\nu}$ converge to the optimal solution $\mathbf{a}^*$, $\boldsymbol{\mu}^*$, and $\boldsymbol{\nu}^*$. The key variables that we will utilize for our proposed retail market mechanism are $P_{\mathbf{j}}^{\mathrm{G}^*}, Q_{\mathbf{j}}^{\mathrm{G}^*}$, $P_{\mathbf{j}}^{\mathrm{L}^*}, Q_{\mathbf{j}}^{\mathrm{L}^*}$, the active and reactive power generation at bus $\mathbf{j}$ and consumption profiles, and $\mu_{\mathbf{j}}^{\mathrm{P}^*}$, $\mu_{\mathbf{j}}^{\mathrm{Q}^*}$, the retail prices. Implementation of the PAC algorithm with the information exchanged between buses is illustrated in Fig. 1.

The next section will discuss the advantages of the PAC algorithm over the dADMM algorithm (see [38] for details).

D. Comparison of PAC and dADMM

There are two main advantages of PAC over the dADMM algorithm. First, the PAC algorithm requires lower computational effort for each update while assuring a comparable convergence rate. Secondly, the PAC algorithm has enhanced privacy preserving characteristics. These two advantages will be discussed below; for more technical details, please refer to [7] which carries out a more complete comparison and analysis.

1) Convergence: The convergence rate of the PAC is similar to the convergence rate of the dADMM, with both algorithms exhibiting sublinear convergence [6], [7]. However, the PAC algorithm is superior to dADMM in that less computational effort is needed at each step for computing primal and dual variables. This can practically lead to faster convergence times, despite requiring the same number of iterations.

2) Privacy: The PAC algorithm is privacy preserving. The cost functions of the DERs, $\mu_{\mathbf{j}}$ which are the retail prices, and the $\nu_{\mathbf{j}}$ which are the coordination costs, all remain private to each atom $\mathbf{j}$. The only outside variables needed at each $\mathbf{j}$ are $\mathbf{a}$ and $\tilde{\nu}_{\mathbf{j}}$, as in Fig. 1. That the cost functions and $\mu_{\mathbf{j}}$ remain private are common to both dADMM and PAC. However, unlike dADMM, the dual variable $\nu_{\mathbf{j}}$ remains private to atom $\mathbf{j}$ in PAC. The dual variable $\nu_{\mathbf{j}}$ can be thought of as a coordination price, indicating how far an atom $\mathbf{j}$ must be from its optimal point in order to achieve coordination and an overall optimal solution for the complete distribution grid. If $\nu_{\mathbf{j}}$ is high, then atom $\mathbf{j}$ is further from its atomic optimal point–thus, $\nu_{\mathbf{j}}$ describes the tension between atomic and network optimality.

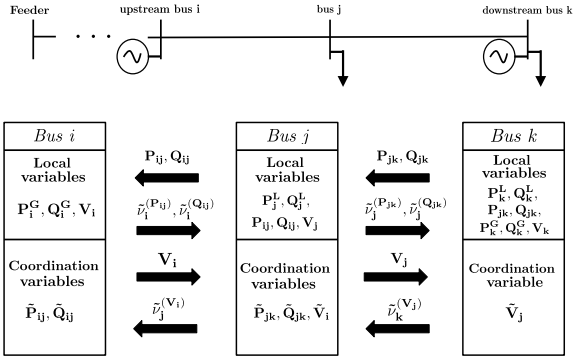

Fig. 1. Illustration of the PAC algorithm and communication between atoms.

The importance of privacy of $\nu_{\mathbf{j}}$ can be explained thus: with knowledge of the $\nu_{\mathbf{j}}$ values, a rogue agent can carry out a cyberattack, deliberately manipulating the variables that are communicated between atoms to be maximally different from one another. This action has two implications: First, it will take longer to converge. Second, since the values are maximally different, each atom $\mathbf{j}$ will be forced further away from its atomic optimal point, incurring "losses" as it tries to coordinate with its neighbors to achieve optimality. The losses can be thought of as an opportunity cost: to meet network constraints, atom $\mathbf{j}$ has to sacrifice revenue it could have received had it been operating closer to atomic optimality. We note that there may be more targeted ways to use the $\mathbf{j}$ values, such as by agents to coerce neighbors into certain behaviours. Thus, by keeping $\nu_{\mathbf{j}}$ private to each atom, the PAC algorithm has added privacy characteristics and may exhibit more resiliency to cyberattacks than dADMM.

III. A Retail Market Mechanism

Our proposed retail market has a Distribution System Operator (DSO) which is designated to carry out transactions in the distribution grid through (1) an energy market and (2) in an ancillary market. A schematic of both the physical layer and the market layer of the proposed retail market is shown in Fig. 2. All data communication coming from the WEM is shown with solid arrows, while data communication moving upstream through the DSO is shown with dashed arrows.

A. Overall Structure of the Retail Market

The DSO is composed of DSO Representatives ($\mathrm{DSO_r}$) and DSO Workers ($\mathrm{DSO_w}$), located at each primary feeder and substation, respectively. The energy market transactions occur at each primary feeder, between the $\mathrm{DSO_r}$ and agents representing DERs at each bus of that feeder. The DERs are assumed to live at the primary feeder level; any DERs and uncontrollable loads at the secondary feeder level and below are represented through aggregators and do not directly participate in this retail market. Thus, each bus $\mathbf{j}$ in the physical

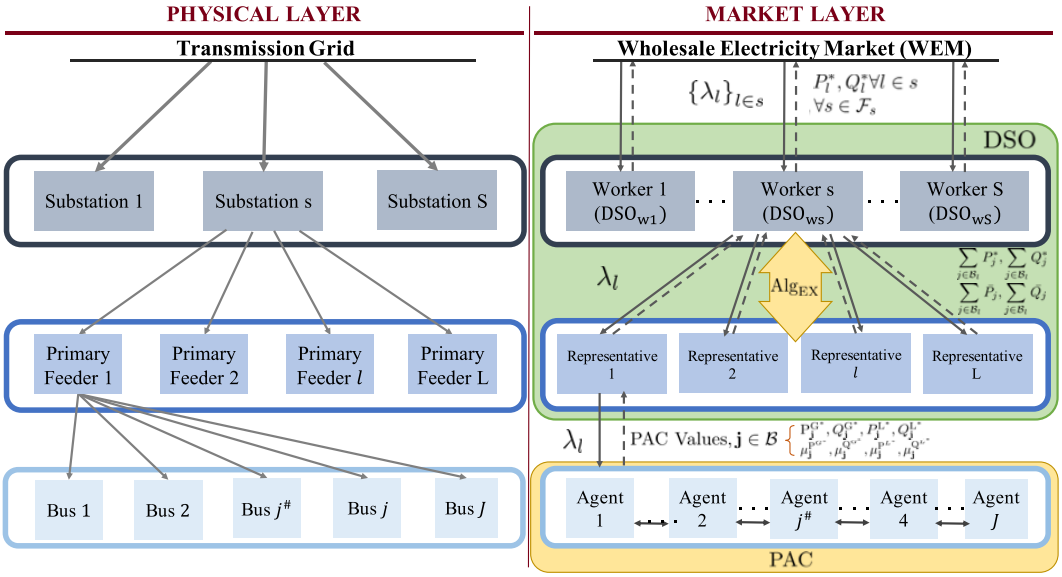

Fig. 2. Proposed retail market structure.

layer is an independent agent in the market layer, acting to minimize its expenses while subjected to network constraints.

Each agent is also an atom $\mathbf{j}$ in the PAC algorithm,[1] which specifies how these agents interact with one another. Agents securely share information so as to converge to the optimal schedules and retail prices (d-LMPs) for each DER. These converged values are the basis of a bilateral agreement between the DSO_r and each agent. The DSO_r is responsible for making payments to the DERs, and charging all agents for their consumption (net their generation).

The DSO_r will then aggregate all data from its agents, and send the aggregated load and generation information to its respective DSO_w. Prior to the next WEM clearing, and under normal grid operation, the DSO_w will convey the net load (or generation) to the WEM. The assumption is that the WEM will accept to serve this net load (accept to receive this net generation). The DSO_w is also responsible for making payments to (or accepting payments from) the WEM for power imported from (or exported to) the transmission grid.

The ancillary services market deals with alert system conditions. Each agent must notify its status of operation to the DSO_r, which aggregates this data and flags any risks of service disruption. In turn, the DSO_r must notify its DSO_w, which monitors the status of all its feeders. Then, the DSO_w will carry out an "emergency procedure", denoted as Alg_EX, to dispatch ancillary units consisting of distributed generators and fast-acting demand response loads, within its feeders. For example, suppose feeder 1 receives an alert status from one of its agents who will no longer be able to generate the amount of power it had committed. Then, through Alg_EX, the DSO_w will find, among the L connected feeders (in $\mathcal{F}_s$), the lowest cost generators to make up the shortfall, or loads to reduce consumption and redirect power to feeder 1. Further details follow.

[1]This one-to-one mapping of agents to atoms is not a requirement of the PAC algorithm, but rather a product of the independence of agents in the market layer.

B. Energy Market

The energy market employs the PAC algorithm to determine the optimal scheduling of $P_\mathbf{j}^{\text{G}*}$, $Q_\mathbf{j}^{\text{G}*}$ of the generating units, $P_\mathbf{j}^{\text{L}*}$, $Q_\mathbf{j}^{\text{L}*}$ of the consumption units, and their d-LMPs $\mu_\mathbf{j}^{\text{P}*}, \mu_\mathbf{j}^{\text{Q}*}$, at node $\mathbf{j}$, for all $\mathbf{j}$ in the distribution grid. We denote ΔT and $\Delta\tau$ to be the market clearing periods of the WEM and the retail market, respectively. For ease of exposition, we assume that $\Delta\tau \ll \Delta T$, so the DSO market clears multiple times within a single WEM clearance period. However, in general, these two clearing periods can be chosen independently.

We make the following additional assumption: Between any two market clearings T_0 and $T_0 + \Delta T$ of the WEM, the LMP of all feeder buses $\lambda_\mathbf{l}^{\text{P}}$ is fixed, for all feeders in a substation. This is denoted compactly as "$\lambda_\mathbf{l}^{\text{P}}$ is fixed, $\forall \mathbf{l} \in \mathcal{F}_s, \forall \mathbf{s} \in \mathcal{S}$". Thus in (2), $\lambda_\mathbf{l}^{\text{P}}$ is a boundary condition $\forall \mathbf{l} \in \mathcal{F}_s, \forall \mathbf{s} \in \mathcal{S}$ on the scheduling problem, for the N DSO clearings over the time period $[T_0, T_0 + \Delta T]$. It should be noted however that in (2), the power quantities $P_\mathbf{j}^G, Q_\mathbf{j}^G$ are allowed to vary, and will be determined by the PAC algorithm, $\forall \mathbf{j} \in \mathcal{B}$.

Note that in PAC, the feeder node $j^\#$ is treated as a generator of infinite capacity ($\overline{P_{j^\#}^{\text{G}}} \gg 0$, where $\overline{P_{j^\#}^{\text{G}}}$ corresponds to the upper limit of power generation from (7)) – thus, $P_{j^\#}^{\text{G}*}$ represents power imported from the main grid. Likewise, $P_{j^\#}^{\text{L}*}$ represents power exported to the main grid. Depending on whether the power is imported or exported, either $P_{j^\#}^{L*} = 0$ or $P_{j^\#}^{G*} = 0$, respectively. Then for time period $[T_0, T_0 + \Delta T]$ the average load (generation) of the distribution grid which will be imported from (exported to) the main grid is calculated as $P_{\mathbf{l},T_0}^* = \frac{1}{N}\sum_{n=1}^{N} P_{j^\#,n}^{\text{G}*} - P_{j^\#,n}^{\text{L}*}$, $\forall \mathbf{l} \in \mathcal{F}_s, \forall \mathbf{s} \in \mathcal{S}$.

With the above assumptions in place we propose that the retail market determines the overall generation, consumption,

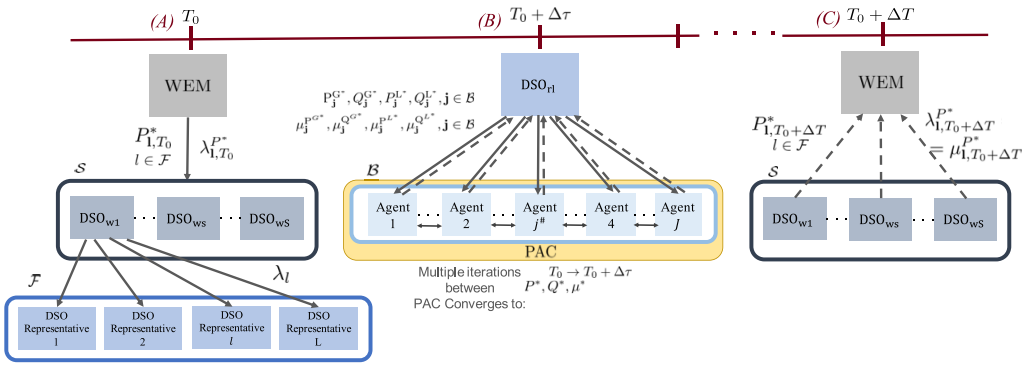

Fig. 3. Timeline of primary market layer interactions.

and prices at each $j \in \mathcal{B}$ in the distribution grid, using the PAC algorithm described in (12)-(18) over every DSO market clearing period $\Delta\tau$. Note that the PAC algorithm is run independently for each feeder.

Fig. 3 shows the interactions between the WEM, DSO, and agents for the proposed energy market over one clearing of the WEM. The energy retail market will consist of three interactions denoted as (A), (B), and (C). The first interaction (A) occurs between the WEM and DSO$_w$s, when the WEM clears: at time T_0 the WEM passes to each DSO$_w$ the forecasted load/generation over the period, and the LMPs for each of its DSO$_r$s, $\mathbf{l} \in \mathcal{F}_s$, $\forall \mathbf{s} \in \mathcal{S}$. This information is passed down to each DSO$_r$, which shares the LMP with its agents. The second set of interactions (B) occur between the DSO$_r$ and the agents every $\Delta\tau$, prior to the next WEM clearing. For each interaction (B), the agents will coordinate amongst each other, through the PAC algorithm, and converge in some K iterations. In doing so, the converged values of the real and reactive power generation and load for each bus, $P^{G^*}_{\mathbf{j}}$, $Q^{G^*}_{\mathbf{j}}$,$P^{L^*}_{\mathbf{j}}$, $Q^{L^*}_{\mathbf{j}}$, in the distribution grid will be determined, along with their respective d-LMPs, $\mu^*_{\mathbf{j}}$. The agents will enter into bilateral contracts with the DSO$_r$ with these scheduled values. The d-LMPs are valid for the period $\Delta\tau$. This interaction repeats until the next WEM clearing. Prior to the next clearing of the WEM, the DSO$_r$ will send to the DSO$_w$ the load to be imported from (exported to) the main grid, $P^*_{\mathbf{l},T_0}$, which has been aggregated over the N DSO clearings. The last interaction (C) from Figure 3, is between the WEM and the DSO$_w$s, and occurs at the next clearing of the WEM, $T_0 + \Delta T$. Each DSO$_w$ will send to the WEM per each feeder, the load to be imported from (exported to) the main grid, $P^*_{\mathbf{l},T_0}$, which has been aggregated over the N DSO clearings.

C. Ancillary Services Market

The sections above detail the market under normal grid operation. Upon receiving an alert status from a DSO$_r$, the ancillary services market is employed, to address the shortfall in generation or load reduction. The alert code, code$_a$, details whether a generator or a demand response resource is no longer capable of generating or reducing demand as committed in the market period, respectively. The DSO$_w$ runs the Alg$_{EX}$ procedure, whereby the optimization problem in (17) is solved to meet the shortfall in feeder x, ΔP_x, while minimizing the cost of deploying ancillary resources. In doing so, the DSO$_w$ leverages the distributed network structure of the connected feeders.

$$\begin{aligned}
\min \quad & \sum_{\mathbf{l}\in\mathcal{F}_s}\left(\mu^{\mathrm{P,G'}}_{\mathbf{l}} P^{\mathrm{G'}}_{\mathbf{l}} + \mu^{\mathrm{P,L'}}_{\mathbf{l}} P^{\mathrm{L'}}_{\mathbf{l}}\right) \\
\text{subject to:} \quad & \sum_{\mathbf{l}\in\mathcal{F}_s}\left(P^{\mathrm{G'}}_{\mathbf{l}} + P^{\mathrm{L'}}_{\mathbf{l}}\right) = \min\left(\Delta P_x, P^{\mathrm{G}^*}_x\right) \\
& P^{\mathrm{G'}}_{\mathbf{l}} \le \overline{P^{\mathrm{G'}}_{\mathbf{l}}} \qquad \forall \mathbf{l} \in \mathcal{F}_s \\
& P^{\mathrm{L'}}_{\mathbf{l}} \le \overline{P^{\mathrm{L'}}_{\mathbf{l}}} \qquad \forall \mathbf{l} \in \mathcal{F}_s \\
& P^{\mathrm{G'}}_{\mathbf{l}}, P^{\mathrm{L'}}_{\mathbf{l}} \ge 0 \qquad \forall \mathbf{l} \in \mathcal{F}_s
\end{aligned} \tag{17}$$

where $P^{\mathrm{G'}}_{\mathbf{l}}$ is the additional generation required from feeder $\mathbf{l}$, and $P^{\mathrm{L'}}_{\mathbf{l}}$ is the additional load reduction required from feeder $\mathbf{l}$ in order to meet the shortfall in feeder x.

In order to run Alg$_{EX}$, the DSO$_w$ requires the following data from each of its DSO$_r$s, regarding their respective distribution networks:

- Maximum generating capacity: $\overline{P^{\mathrm{G}}_{\mathbf{l}}} = \sum_{\mathbf{j}\in\mathcal{B}_{\mathbf{l}}\setminus j^\#} \overline{P^{\mathrm{G}}_{\mathbf{j}}}$;
- Minimum load requirement: $\underline{P^{\mathrm{L}}_{\mathbf{l}}} = \sum_{\mathbf{j}\in\mathcal{B}_{\mathbf{l}}} \underline{P^{\mathrm{L}}_{\mathbf{j}}}$;
- Optimal generation set point, as determined by PAC and committed in the primary market: $P^{\mathrm{G}^*}_{\mathbf{l}} = \sum_{\mathbf{j}\in\mathcal{B}_{\mathbf{l}}\setminus j^\#} P^{\mathrm{G}^*}_{\mathbf{j}}$;
- Optimal load set point, as determined by PAC and committed in the primary market: $P^{\mathrm{L}^*}_{\mathbf{l}} = \sum_{\mathbf{j}\in\mathcal{B}_{\mathbf{l}}} P^{\mathrm{L}^*}_{\mathbf{j}}$;
- Weighted average cost of local distributed generation: $\mu^{\mathrm{P,G'}}_{\mathbf{l}} = \frac{\sum_{\mathbf{j}\in\mathcal{B}_{\mathbf{l}}\setminus j^\#} \mu^{\mathrm{P}^*}_{\mathbf{j}} \overline{P^{\mathrm{G}}_{\mathbf{j}}}}{\sum_{\mathbf{j}\in\mathcal{B}_{\mathbf{l}}\setminus j^\#} \overline{P^{\mathrm{G}}_{\mathbf{j}}}}$;
- Weighted average cost of using demand response: $\mu^{\mathrm{P,L'}}_{\mathbf{l}} = \frac{\sum_{\mathbf{j}\in\mathcal{B}_{\mathbf{l}}\setminus j^\#} \mu^{\mathrm{P}^*}_{\mathbf{j}} (\overline{P^{\mathrm{L}}_{\mathbf{j}}} - \underline{P^{\mathrm{L}}_{\mathbf{j}}})}{\sum_{\mathbf{j}\in\mathcal{B}_{\mathbf{l}}\setminus j^\#} (\overline{P^{\mathrm{L}}_{\mathbf{j}}} - \underline{P^{\mathrm{L}}_{\mathbf{j}}})}$;
- Alert information: [code$_a$ ΔP_x], where ΔP_x is the change in power quantity - either a decrease in generation capabilities, or a decrease in demand response capabilities (i.e., increase in $\underline{P^{\mathrm{L}}_{\mathbf{j}}}$ for some $\mathbf{j}$ in feeder x). We note $\Delta P_x > 0$.

The Alg$_{EX}$ procedure is described next for generation shortfall, and a similar procedure is carried out for the other alert code. For ease of exposition, suppose DSO$_r$ 1 sends an alert code of 0 with a shortfall quantity of ΔP_1. The new maximum generation capacity for the feeder is then $\overline{P^{\mathrm{G}}_{\mathbf{l},\Delta}} = \overline{P^{\mathrm{G}}_{\mathbf{l}}} - \Delta P_1$. Under this shortfall, the committed generation must also be adjusted, $P^{\mathrm{G}^*}_{\mathbf{l},\Delta} = P^{\mathrm{G}^*}_{\mathbf{l}} - \Delta P_1$. The DR capabilities remain the

same. Finally, the new uncommitted generation and DR limits for the feeder can be calculated as $\overline{P_{\mathbf{l}}^{\mathrm{G}'}} = \overline{P_{\mathbf{l},\Delta}^{\mathrm{G}}} - P_{\mathbf{l},\Delta}^{\mathrm{G}^*}$ and $\overline{P_{\mathbf{l}}^{\mathrm{L}'}} = P_{\mathbf{l}}^{\mathrm{L}^*} - \underline{P_{\mathbf{l}}^{\mathrm{L}}}$ respectively.

D. DSO Revenue

With the market structure as described above, we can determine the DSO's net revenue as follows:

$$\mathcal{P}_{\mathrm{DSO}} = \mathcal{R}_{\mathrm{DSO}}^{\mathrm{L}} - \mathcal{C}_{\mathrm{DSO}}^{\mathrm{flex}} - \mathcal{C}_{\mathrm{DSO}}^{\mathrm{DG}} - \mathcal{C}_{\mathrm{DSO}}^{\mathrm{WEM}} \tag{18}$$

with the different components that contribute to the net revenue defined as follows:

- Revenue earned from all loads: $\mathcal{R}_{\mathrm{DSO}}^{\mathrm{L}} = \sum_{j\in\mathcal{B}}(\mu_{\mathbf{j}}^{\mathrm{P}^*} P_{\mathbf{j}}^{\mathrm{L}^*} + \mu_{\mathbf{j}}^{\mathrm{Q}^*} Q_{\mathbf{j}}^{\mathrm{L}^*})$
- Payments made to flexible loads: $\mathcal{C}_{\mathrm{DSO}}^{\mathrm{flex}} = \sum_{j\in\mathcal{B}}(\mu_{\mathbf{j}}^{\mathrm{P}^*}(P_{\mathbf{j}}^{\mathrm{L}0} - P_{\mathbf{j}}^{\mathrm{L}^*}) + \mu_{\mathbf{j}}^{\mathrm{Q}^*}(Q_{\mathbf{j}}^{\mathrm{L}0} - Q_{\mathbf{j}}^{\mathrm{L}^*}))$
- Payments made to distributed generators: $\mathcal{C}_{\mathrm{DSO}}^{\mathrm{DG}} = \sum_{j\in\mathcal{B}\setminus j^{\#}}(\mu_{\mathbf{j}}^{\mathrm{P}^*} P_{\mathbf{j}}^{\mathrm{G}^*} + \mu_{\mathbf{j}}^{\mathrm{Q}^*} Q_{\mathbf{j}}^{\mathrm{G}^*})$
- Payment made to WEM, for purchasing power: $\mathcal{C}_{\mathrm{DSO}}^{\mathrm{WEM}} = \lambda_{\mathbf{l}}^{\mathrm{P}} P_{\mathbf{l}}^{\mathrm{G}^*} + \lambda_{\mathbf{l}}^{\mathrm{Q}} Q_{\mathbf{l}}^{\mathrm{G}^*}$

To evaluate this net revenue, we set up a benchmark system which consists of a utility that purchases power from the WEM and sells to customers at a retail price, $\lambda_{\mathrm{retail}}^{\mathrm{P}}$. In this system, DERs are assumed to not be compensated for their services, as they are small-scale behind-the-meter resources. Thus, the DSO's profit *without* the retail market is:

$$\mathcal{P}_{\text{no-DSO}} = \mathcal{R}_{\text{no-DSO}}^{\mathrm{L}} - \mathcal{C}_{\text{no-DSO}}^{\mathrm{WEM}} \tag{19}$$

where the first term denotes the revenue earned from all loads, given by

$$\mathcal{R}_{\text{no-DSO}}^{\mathrm{L}} = \lambda_{\mathrm{retail}}^{\mathrm{P}} \sum_{j\in\mathcal{B}} P_{\mathbf{j}}^{\mathrm{L}^*} + \lambda_{\mathrm{retail}}^{\mathrm{Q}} \sum_{j\in\mathcal{B}} Q_{\mathbf{j}}^{\mathrm{L}^*}$$

and the payment to the WEM is

$$\mathcal{C}_{\text{no-DSO}}^{\mathrm{WEM}} = \lambda_{\mathbf{l}}^{\mathrm{P}} P_{\mathbf{l}}^{\mathrm{G}^*} + \lambda_{\mathbf{l}}^{\mathrm{Q}} Q_{\mathbf{l}}^{\mathrm{G}^*}$$

From (18)-(19), it follows that the additional revenue earned by the DSO when using the retail market mechanism is given:

$$\mathcal{P}_{\text{DSO-increase}} = \mathcal{P}_{\mathrm{DSO}} - \mathcal{P}_{\text{no-DSO}} \tag{20}$$

Similarly, we can also quantify the savings for an inflexible consumer, j as

$$\mathcal{P}_{\text{consumer-saving}} = (\lambda_{\mathrm{retail}}^{\mathrm{P}} - \mu_{\mathbf{j}}^{\mathrm{P}^*}) P_{\mathbf{j}}^{\mathrm{L}^*} \tag{21}$$

and we note that flexible consumers will receive additional compensation in the form of revenue for their services.

As mentioned earlier, we propose that this retail market clears every $\Delta\tau$ seconds. We group a 24-hour period into 24 hour-long intervals $T_i = [i, i+1]$, where i corresponds to the ith hour, $i = 0, \ldots, 23$, over this 24 hour period. Suppose that over this T_i, there are N clearings of the retail market, which occur at $t = i + n\Delta\tau$, $n = 1, \ldots, N$, and M clearings of the WEM, which occur at $t = i + m\Delta T$, $m = 1, \ldots, M$. Since $\Delta\tau \ll \Delta T$, it follows that $n > m$. Denoting $n' = i + n\Delta\tau$ and $m' = i + m\Delta T$, we can then represent the profit calculated above as a function of time:

$$\mathcal{P}_{\text{DSO-increase}}(i) = \sum_{n=1}^{N} \big(\mathcal{P}_{\mathrm{DSO}}(n', m') - \mathcal{P}_{\text{no-DSO}}(n', m')\big) \tag{22}$$

where the n' is carried through to the $\mu_{\mathbf{j}}$, $P_{\mathbf{j}}$, and $Q_{\mathbf{j}}$, and the m' is carried through to the $\lambda_{\mathbf{l}}$, $\lambda_{\mathrm{retail}}$, and $P_{\mathbf{l}}$.

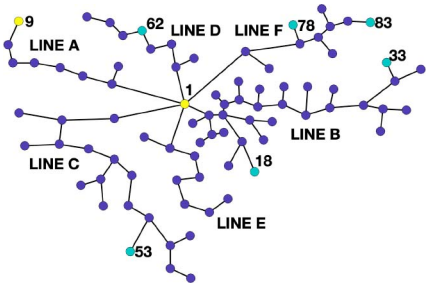

Fig. 4. An illustration of the distribution network model. The filled circles show the nodes $\mathcal{B}$. The blue, yellow, and teal filled circles indicate loads, local generators and both, respectively.

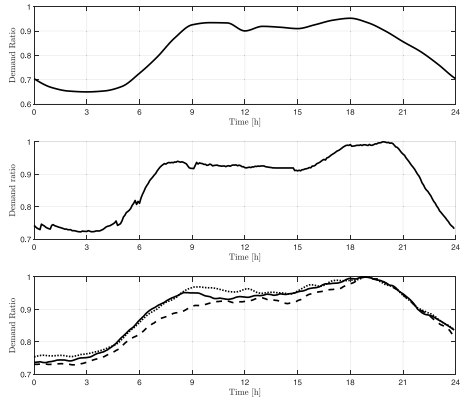

Fig. 5. The profiles of the time-dependent demand ratio $\alpha(i)$, $i = 0, \ldots, 24$, for Networks JST-CREST 126 (top), IEEE-123 (middle), and modified IEEE-13 (bottom).

IV. Numerical Experiments

Simulations were carried out on three networks. The market under normal operation was tested on a real distribution network in Tokyo, Japan, and a modified IEEE 123-bus network. The market under the alert case was tested with an illustrative multi-feeder network, composed of modified three IEEE 13-bus networks. Simulations were carried out over a 24 hour period (i varies between 0h and 23h). The baseline $P_{\mathbf{j}}^{\mathrm{L}\,0}(i)$ at the ith hour is defined as $P_{\mathbf{j}}^{\mathrm{L}\,0}(i) \triangleq \alpha(i)\overline{P_{\mathbf{j}}^{\mathrm{L}}}$ where the time-dependent ratio $\alpha(i)$ varies differently for each network.

A. Network 1: JST-CREST 126 Distribution Feeder Model

The original network model, presented in detail in [39], represents a distribution grid in Komae city in Tokyo, Japan with an area of 5 km^2. Here we employ a compressed version of that network, shown in Fig. 4. Our model contains $|\mathcal{B}| = 84$ nodes and 6 lines all connected to the feeder node in a star topology. Details of base values and parameters are provided

TABLE I
SIMULATION PARAMETERS FOR NETWORKS 1-3

Parameter	JST-CREST 126	IEEE 123	3 feeder (per network)
$\lvert\mathcal{B}\rvert$	84	123	13
$\lvert\mathcal{T}\rvert$	83	122	12
f_{base}, Hz	50	60	60
v_{base}, kV	6.6	4.16	4.16
S_{base}, kVA	10^3	10^3	10^3
$\underline{v_{\mathbf{j}}}$, pu	0.95	0.8	0.9
$\overline{v_{\mathbf{j}}}$, pu	1.05	1.2	1.1
$\overline{S^2_{\mathbf{i},\mathbf{j}}}$, pu	2	10	10
$\overline{Q^{\text{G}}_{\mathbf{j}}}, -\underline{Q^{\text{G}}_{\mathbf{j}}}$	$0.15\overline{P^{\text{G}}_{\mathbf{j}}}$	See [45]	See [45]
$\underline{P^{\text{G}}_{\mathbf{j}}}$	0	0	0
$\overline{P^{\text{L}}_{\mathbf{j}}}$	0	0	0
$\overline{\overline{Q^{\text{L}}_{\mathbf{j}}}}$	0	See [45]	See [45]
$\underline{Q^{\text{L}}_{\mathbf{j}}}$	0	0	0
$\beta^{\text{PL}}_{\mathbf{j}}$		$\in [400, 800]$	
$\beta^{\text{PG}}_{\mathbf{j}}$		$\in [4, 8]$	
$\beta^{\text{QG}}_{\mathbf{j}}$		$\in [4, 8]$	
ξ		100	
$\lambda^{\text{Q}}_{\mathbf{1}}$		1	

TABLE II
LINE AND LOAD NODE DATA

LINE	A	B	C	D	E	F
Nodes in $\tilde{\mathcal{B}}$	8	31	18	8	8	10
Branches in $\mathcal{T}$	1	14	6	1	1	4
Total # of loads $\mathbf{j}$	4	17	12	4	4	6
Sum of $\overline{P^{\text{L}}_{\mathbf{j}}}$ [MW]	0.84	3.56	2.51	0.84	0.84	1.26

TABLE III
GENERATION NODE DATA FOR JST-CREST 126

$j \in \mathcal{B}$	1	9	18	33	53	62	78	83
$\overline{P^{\text{G}}_{\mathbf{j}}}$ [MW]	10	5	0.6	1.2	0.6	0.3	1.8	3
$\overline{P^{\text{L}}_{\mathbf{j}}}$ [MW]	0	0	0.14	0.08	0.31	0.08	0.32	0.07

TABLE IV
GENERATION NODE DATA FOR IEEE 123

$j \in \mathcal{B}$	1	25	40	67	81	94
$\overline{P^{\text{G}}_{\mathbf{j}}}$ [MW]	20	0.5	0.7	0.8	1.2	0.75

in Table I, with base values determined as typical to power systems in Japan [40]. Information on electrical lines/loads and generators can be found in Table II and Table III, respectively. The parameters $\overline{P^{\text{L}}_{\mathbf{j}}}$ are obtained randomly, to satisfy the total upper capacity values in Table II. The time-dependent ratio $\alpha(i)$ varies according to the FY2017 average consumption profile in the Tokyo area [41]. The 24-hour profile of $\alpha(\tau)$ is shown in Fig. 5 (top). In addition, $v_1 = 1.023$ pu (with nominal value 6750V), and all loads are taken as unity power factor loads. We assume that the reactive power of flexible consumers can be adjusted through proper control of the air-conditioners. Further, we assume the P-LMP, $\lambda^{\text{P}}_{\mathbf{1}}$, is either fixed at 10 or is time-varying and varies according to the yearly average profile of the FY2017 system price in Japan Electric Power eXchange (JEPX) [42] as shown in Fig. 6 (top) The retail price for electricity is fixed at 26 JY/kWh, as per average retail electricity prices in Japan [43], [44].

TABLE V
GENERATION NODE DATA FOR IEEE 13

Feeder 1	$j \in \mathcal{B}$	1	4	10	13
	$\overline{P^{\text{G}}_{\mathbf{j}}}$ [MW]	40	0.8	0.5	0.3
Feeder 2	$j \in \mathcal{B}$	1	5	8	12
	$\overline{P^{\text{G}}_{\mathbf{j}}}$ [MW]	40	1	1.5	1.5
Feeder 3	$j \in \mathcal{B}$	1	10	8	
	$\overline{P^{\text{G}}_{\mathbf{j}}}$ [MW]	40	2	0.25	

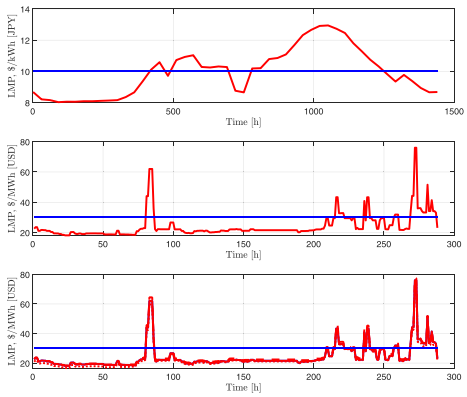

Fig. 6. Profiles of P-LMP $\lambda^{\text{P}}_{\mathbf{1}}$ where red denotes the yearly average profile and blue a constant LMP, for Networks JST-CREST 126 (top), IEEE-123 (middle), and modified IEEE-13 (bottom).

B. Network 2: Modified IEEE 123 Model

The IEEE 123 bus network was modified to be a balanced 3-phase distribution network as below:

- switches were assumed in their normal positions
- single-phase spot loads were assumed to be 3-phase
- cables were assumed to be 3-phase transposed, with configurations 1 thru 12 converted to symmetric matrices
- shunt capacitors were modeled as reactive power generators, and were assumed to be 3-phase

Information on electrical line/loads and generators can be found in IEEE documentation [45]. Further details are provided in Table I and generator data can be found in Table IV. The time-dependent ratio $\alpha(i)$ is deduced from the ISO-NE report of total recorded electricity demand for each five-minute interval of May 14, 2019 [46], as shown in Fig. 5 (middle). Loads are not assumed to be unity power factor. Finally, we assume the P-LMP, $\lambda^{\text{P}}_{\mathbf{1}}$, is either fixed at \$30/MWh or is time-varying and varies according to the ISO-NE report of the final approved LMPs for each five-minute interval for May 14, 2019 [47], as shown in Fig. 6 (middle).

C. Network 3: 3 Feeder Modified IEEE 13 Model

To test the alert case, a multi-feeder network was developed, with $|\mathcal{F}_s| = 3$ and $|\mathcal{B}_{\mathbf{l}}| = 13 \forall \mathbf{l} \in \mathcal{F}_s$. The IEEE 13-bus network [45] was modified to be balanced 3-phase (as for Network 2). Variations of the network were developed by adding generators of varying capacity at different locations (see Table V), and perturbing the base loads as $\overline{P^{\text{L}}_{\mathbf{j}}} \triangleq \overline{P^{\text{L}}_{\mathbf{j}}}(1 + \delta_{\mathbf{j}})$, where $\delta_{\mathbf{j}} \sim \mathcal{N}(0, 0.15) \forall \mathbf{j} \in \mathcal{B}_{\mathbf{l}}, \forall \mathbf{l} \in \mathcal{F}_s$. The time-dependent ratio *per feeder*, $\alpha_{\mathbf{l}}(i)$, is obtained by perturbing the ISO-NE demand report [46] from May 14, 2019 as

TABLE VI
COMPUTATIONAL DELAYS AND LATENCY REQUIREMENTS

SINGLE COMPUTATIONS	Market Agent(s)	Time (s)
Data Processing: aggregating agent data	DSO_r	5
Data Processing: check for 'alert' system status	DSO_w	5
Algorithm Execution: run Alg_{EX}	DSO_w	10
LATENCY REQUIREMENTS	**Market Agent(s)**	**Time (s)**
Data communication: at PAC convergence	Agents $\rightarrow$ DSO_r	1
Data communication: before next market clearing	DSO_r $\rightarrow$ DSO_w	15

TABLE VII
PAC COMPUTATIONAL TIME

PAC COMPUTATION PER ITERATION k	Market Agent(s)	Time (s)	No. Iterations	Total Time (s)
Algorithm Execution	Atom	0.0092	4500	41.4473
PAC information exchange (latency requirement)	Atom $j \leftrightarrow$ Atom i	0.1	4499	449.9
Total PAC Computational Time				491.35

$\alpha_{\mathbf{l}}(i) = \alpha(i)\delta_{\mathbf{l}}$, where $\delta_{\mathbf{l}} \sim \mathcal{N}(0, 0.075)$ and smoothing the resulting profile. The three demand curves are shown in Fig. 5 (bottom). The feeder P-LMPs, $\lambda^{\mathrm{P}}_{\mathbf{l}}$, are either fixed at \$30/MWh or are time-varying and varies according to the ISO-NE five-minute LMPs for May 14, 2019 [47], taken from different location IDs for each feeder, $\mathbf{l} \in \mathcal{F}_s$ as shown in Fig. 6 (bottom).

D. Performance Evaluation of Algorithm

Initial numerical simulations were conducted on a 2.6GHz CPU Intel Core i7-5600U PC using MATLAB and CVX. To improve performance, the algorithm was then implemented using MATLAB, with optimization problems being setup using the YALMIP interface, and solved directly with Gurobi Optimizer. These simulations were conducted on a 3.00GHz CPU Intel Xeon E5-1660 v3, 8 core workstation, with 128GB RAM. The analysis below was conducted for Network 1; similar results can be shown for Networks 2 and 3.

1) Preliminary Analysis: The parameters ρ, $\gamma_{\mathbf{j}}$, and $\hat{\gamma}_{\mathbf{j}}$ of the PAC algorithm were tuned to guarantee convergence of the PAC algorithm (for more details see [6], [7] and Appendix B) and the vector $\mathbf{a}$ was initiated at the optimal solution of the asoROPF (7) at i = 19h. The PAC algorithm was compared with the popular dADMM [38], [48] algorithm to solve Problem (7). Both algorithms were run for 200 iterations, and results are shown in Fig. 7, where the black graph shows the optimal cost of (1) obtained using a centralized optimization solver. Both algorithms converge to a near-optimal value in roughly 150 iterations, with the PAC algorithm converging slightly faster. From the initial implementation using MATLAB/CVX, the total time required to complete 200 iterations with PAC is 130s (0.65s/iteration/atom) and with dADMM is 203s (1.01s/iteration/atom). Hence, when the initial conditions are initiated close to the optimal solution, the proposed PAC algorithm can converge in less than 5 minutes which is the standard time between two WEM clearings.

2) Implementation Considerations: The improved implementation considered the fact that the grid topology can be assumed to be fixed; thus, the constraint matrices, $\tilde{\mathbf{G}}_{\mathbf{j}}$ and $\mathbf{A}_{\mathbf{j},-}$ in the asoROPF (7) are constant. Only the cost function must be updated for each PAC iteration, and the inequality

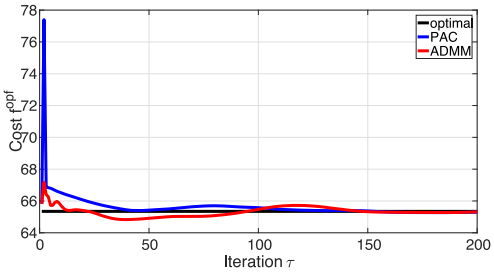

Fig. 7. Cost evolution with PAC and dADMM.

constraints (limits on power generation and load) updated for each time period. For worst-case computational time, the vector $\mathbf{a}$ was initiated at 'zero' - all node variables are initiated at their lower bounds ($\underline{P^{\mathrm{G}}_{\mathbf{j}}}, \underline{P^{\mathrm{L}}_{\mathbf{j}}}, \underline{Q^{\mathrm{G}}_{\mathbf{j}}}, \underline{Q^{\mathrm{L}}_{\mathbf{j}}}, \underline{V_{\mathbf{j}}}$); all line variables are initiated at 0. To guarantee convergence, we run PAC for 4500 iterations. Tables VI and VII provide a summary of estimated computational times and latencies associated with PAC that would correspond to a parallel implementation. Latency is defined as the time between data generation and when it is acted upon by the next agent [49]. We also differentiate between latency and computational delays, which are times associated with application/script execution [49]–[51]. References [49]–[51] were used to obtain reasonable approximations for latencies and computational delays.

These tables show that the retail market completes execution in 8.8 minutes. We expect this time to be reduced by an order of magnitude through better initialization (not zero). For example, a reduction of iterations from 4500 to 450 will reduce execution time from 8.8 to 1.4 minutes. Execution time can be further reduced as latency requirements reduce, to say 0.76 minutes, for 10ms latency compared to 100ms, at 450 iterations.

E. Performance Evaluation of Proposed Market

We benchmark our results using the following scenarios: (1) When all the loads in the distribution grid are served only by the main grid, and (2) when the retail market dispatches DERs through the PAC algorithm with the LMP being either (a)fixed or (b)time varying (see Fig. 6).

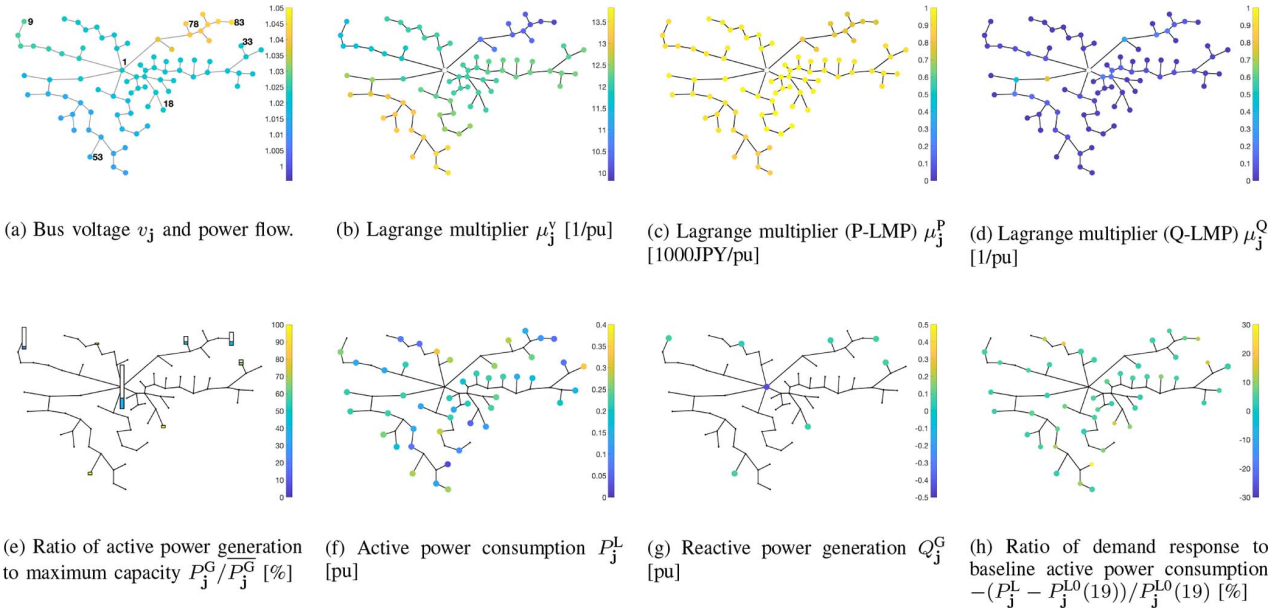

(a) Bus voltage v_{j} and power flow. (b) Lagrange multiplier $\mu_{\mathrm{j}}^{\mathrm{v}}$ [1/pu] (c) Lagrange multiplier (P-LMP) $\mu_{\mathrm{j}}^{\mathrm{P}}$ [1000JPY/pu] (d) Lagrange multiplier (Q-LMP) $\mu_{\mathrm{j}}^{\mathrm{Q}}$ [1/pu]

(e) Ratio of active power generation to maximum capacity $P_{\mathrm{j}}^{\mathrm{G}}/\overline{P_{\mathrm{j}}^{\mathrm{G}}}$ [%] (f) Active power consumption $P_{\mathrm{j}}^{\mathrm{L}}$ [pu] (g) Reactive power generation $Q_{\mathrm{j}}^{\mathrm{G}}$ [pu] (h) Ratio of demand response to baseline active power consumption $-(P_{\mathrm{j}}^{\mathrm{L}} - P_{\mathrm{j}}^{\mathrm{L0}}(19))/P_{\mathrm{j}}^{\mathrm{L0}}(19)$ [%]

Fig. 8. Terminal configurations with the PAC algorithm and time-variant P-LMP $\lambda_{\mathbf{1}}^{\mathrm{P}}$.

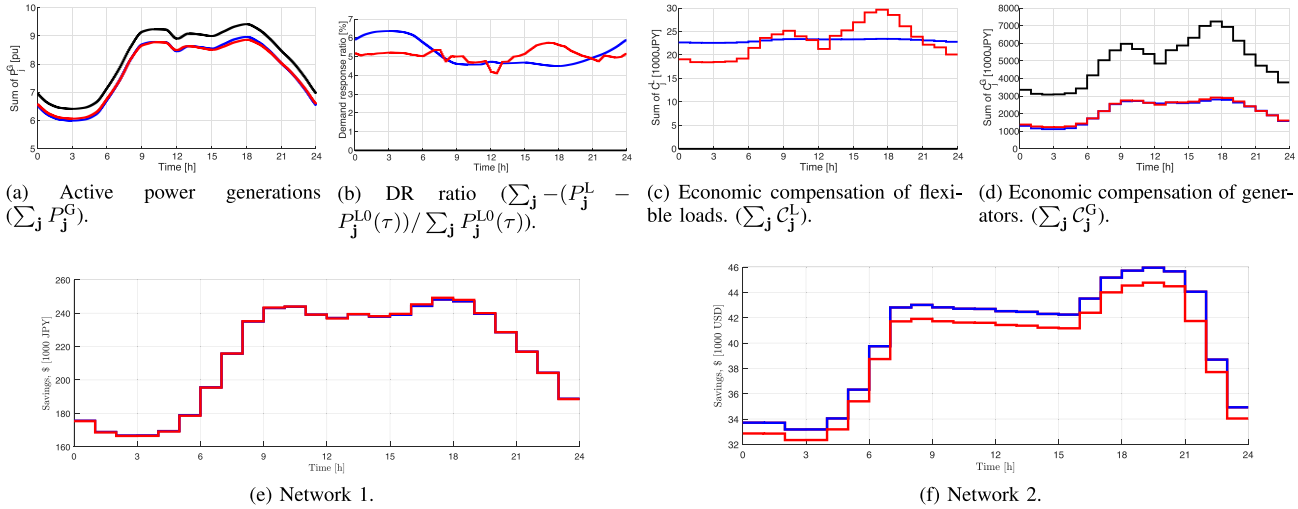

(a) Active power generations $(\sum_{\mathrm{j}} P_{\mathrm{j}}^{\mathrm{G}})$. (b) DR ratio $(\sum_{\mathrm{j}} -(P_{\mathrm{j}}^{\mathrm{L}} - P_{\mathrm{j}}^{\mathrm{L0}}(\tau))/\sum_{\mathrm{j}} P_{\mathrm{j}}^{\mathrm{L0}}(\tau))$. (c) Economic compensation of flexible loads. $(\sum_{\mathrm{j}} \mathcal{C}_{\mathrm{j}}^{\mathrm{L}})$. (d) Economic compensation of generators. $(\sum_{\mathrm{j}} \mathcal{C}_{\mathrm{j}}^{\mathrm{G}})$.

(e) Network 1. (f) Network 2.

Fig. 9. The projected savings from the proposed retail market over a 24-hour period for Networks 1 and 2.

Without loss of generality, we consider bus 1 to be the feeder, $j^{\#} = 1$. For Networks 1 and 2, we assume that the DSO services only this network, i.e., there is a single substation ($\mathcal{S} = \{1\}$) supplying a single feeder ($\mathcal{F} = \{1\}$); thus for brevity, the hierarchy of Fig. 2 can be collapsed. For Network 3, we assume the DSO services only a single substation to which the three feeders are connected. Finally, we assume that $\Delta T = 5$min for all networks, and that $\Delta\tau = 1$min for Network 1, and $\Delta\tau = 5$min for Networks 2 and 3. Thus for Network 1, $N = 60$ and $M = 12$, and Networks 2 and 3 $N = M = 12$ for a single hour of market operation.

1) Results of Network 1: The results from PAC across the distribution grid are shown in Fig. 8. Figure 8(a) shows the voltages across lines A and F are higher than across other lines in the network. This is reasonable as the generation from local generators exceeds the local demand of the loads. Similarly, the voltages across line C are suppressed as the total load connected to line C is higher than the local generated power at node 53. Figure 8(b) shows that the Lagrange multipliers corresponding to the voltage equality constraint, $\mu_{\mathbf{j}}^{V}$, tend to be lower for nodes with higher voltages and vice versa. The local active generation and consumption of the distribution grid can be seen in Fig. 8(e) and Fig. 8(f), and the reactive power generation and demand response throughout the network can be seen in Fig. 8(g) and Fig. 8(h).

To evaluate the impact of the retail market, we compare Scenario (1) and (2), running the PAC algorithm using both LMP profiles shown in Fig. 6. Figure 9(a) shows that generation and electricity imports are lower for Scenario (2), using the market mechanism. Specifically, the DR units are sharing some of the load. This is also illustrated in Fig. 9(b) which shows that DR units accommodate about 5 to 6% of the total load.

The most important results from the proposed market mechanism are the compensation of DER units, and the increase in

TABLE VIII
WEIGHTED AVERAGE COST OF USING DGS OR DRS FOR EACH FEEDER

Item	Feeder 1	Feeder 2	Feeder 3
$\mu_1^{\mathrm{P,G}'}$	0.8811	0.8027	0.7818
$\mu_1^{\mathrm{P,L}'}$	0.8612	0.8194	0.8361

TABLE IX
NEW DISPATCH SETTINGS FROM $\mathrm{Alg_{EX}}$

Item	Feeder 1	Feeder 2	Feeder 3
$P_1^{\mathrm{G}'}$	0	0.3505	0
$P_1^{\mathrm{L}'}$	0	0	0

revenue for the DSO. The DSO's hourly cost for compensating flexible loads and generating units is shown in Fig. 9(c) and 9(d). Note that Scenario (1) assumes no scheduling or compensation of DERs in the network. Figure 9(d) shows a lower total cost for electricity when using the proposed market, as the PAC algorithm optimally schedules the DERs to minimize network costs. Specifically, DERs are used more when electricity prices are higher - the DR units peak usage is around hours 15-18, when the time-varying LMP is the highest.

The hourly increase in revenue obtained from implementing the proposed retail market is shown in Fig. 9(e), using the DSO revenue metric introduced in (22). The revenue earned by the DSO without the retail market is driven by the difference in wholesale and retail price; thus, when the wholesale price of electricity is low, such as during the hours of 1-5, the revenue is high. Compared to the retail cost (26 JY/kWh), the retail market d-LMPs, $\mu_{\mathbf{j}}^{\mathrm{P}*}$, are much lower, thus the increase in revenue is small during hours 1-5. However, as LMPs rise and DERs are efficiently scheduled, the DSO generates additional revenue despite the added costs from compensating the DERs for their services. At the end of the day when the LMP is lower but network demand is high, the retail market continues to make additional revenue. This corroborates the fact that the proposed local retail market can result in lower overall generation cost for serving a given load by efficiently dispatching DG and DR units through the distributed PAC algorithm.

2) Results of Network 2: The proposed market mechanism was also evaluated on the IEEE 123 network. As in the JST-CREST 126 network, the retail market results in an increase in revenue for the DSO, as seen in Fig. 9(f). The increase in revenue is similar to Fig. 9(e), as the demand profiles are very similar. The increase in revenue is lowest during the first 5 hours, where the LMP and demand are both low, and increases as demand increases. The usage of DGs also follows the demand curve, while the demand response ratio is relatively constant over the 24 hours at 6.5%. In this way, PAC makes use of the DGs during periods of higher electricity prices and demand, to lower the network cost of generation. Another key observation is that during the high demand hours of 17-21 where the electricity prices are more volatile, the DSO revenue profile is still smooth, from efficient DER management.

3) Results of Network 3: The proposed ancillary market was evaluated on the 3 feeder modified IEEE 13 network. The PAC algorithm was used to calculate the optimal DR schedule, based on the demand and LMP profiles in Figs. 5 and 6. A contingency was then initiated, whereby feeder 3 loses all generating capabilities ($\Delta P_3 = 2.25$ MW at $T = 230$), some of which was committed. Upon receiving the alert from $\mathrm{DSO_r} = 3$,the $\mathrm{DSO_w}$ carries out $\mathrm{Alg_{EX}}$ (17). The weighted average cost calculated by each $\mathrm{DSO_r}$ is shown in Table VIII. The resulting additional generation or load reduction needed is shown in Table IX. In this test case, feeder 2 has the lowest cost and picks up the slack from feeder 3. If the generating capacity of feeder 2 was all committed, then the DR units in feeder 2 would be deployed, followed by DR units in feeder 3, and so on. The additional cost to the network, based on the weighted average costs is 0.2813 units.

V. CONCLUDING REMARKS

In this paper, we introduce a retail market structure for optimally scheduling DERs in a distribution grid. By leveraging the recently developed distributed PAC algorithm, we designed the retail market with settlement rules that dictate the compensation to DERs and charges to consumers. The effectiveness and performance of the proposed market were evaluated via numerical experiments. The results show the potential of the proposed structure to reduce cost of electricity and increase revenue for the DSO, while enabling market participation for DERs in the distribution grid.

The proposed market structure and interactions (A)-(C) outlined in Section III have assumed that the WEM specifies the LMP $\lambda_{\mathbf{j}}^P$ at T_0 but that the DSO is free to determine the net generation and load seen by the WEM. In practice, the DSO may be obligated to purchase power quantities $P_{\mathbf{l},T_0}^{\mathrm{G}*}, Q_{\mathbf{l},T_0}^{\mathrm{G}*}$ (assuming the DSO is importing power) over the period $[T_0, T_0 + \Delta T]$. In such an event, the proposed PAC can still be used, but with an additional boundary condition: between any two WEM market clearings T_0 and $T_0 + \Delta T$, the net power from the main grid, $P_{\mathbf{l},T_0}^*$ is constant, $\forall \mathbf{l} \in \mathcal{F}_s, \forall \mathbf{s} \in \mathcal{S}$. Thus in interaction (B), the new boundary condition will fix both the LMP $\lambda_{\mathbf{j}}^P$ and power $P_{j\#}^{\mathrm{G}*}, Q_{j\#}^{\mathrm{G}*}$ such that the relevant feeder cost function terms in (2)-(3) are constant for all DSO clearings at $[T_0 + i\Delta\tau, T_0 + (i+1)\Delta\tau], i \in [0, N-1]$.

Additionally, distribution grids are typically meshed and unbalanced. The current formulation of (1) employs a convex relaxation assuming balanced radial networks. However, the PAC algorithm and market structure can be readily extended to these networks by using current injection models. The distributed architecture also suggests an ability to self-recover from cyber-events, such as cyber-attacks or communication network failures. The robustness of the PAC algorithm under these events must be investigated, by using multiple processing units and secure communication protocols. Future work will address these extensions.

APPENDIX A
PAC ALGORITHM DESIGN

We start with the Lagrangian of (9) given by:

$$\mathcal{L}(\mathbf{a}, \boldsymbol{\mu}, \boldsymbol{\nu}) = \sum_{\mathbf{j}\in\mathcal{B}} \Big[\hat{F}_{\mathbf{j}}(\mathbf{a_j}) + \boldsymbol{\mu}^T \tilde{\mathbf{G}}_{\mathbf{j}} \mathbf{a_j} + \boldsymbol{\nu}^T \mathbf{A}_{-,\mathbf{j}} \mathbf{a_j} \Big] \triangleq \sum_{\mathbf{j}\in\mathcal{B}} \mathcal{L}_{\mathbf{j}}(\mathbf{a_j}, \boldsymbol{\mu}_{\mathbf{j}}, \boldsymbol{\nu}).$$

We note that the two variables that are of most importance are $\mathbf{a}$, the decision variable, which corresponds to the optimal power generation and consumption of active and reactive power, and μ, the price associated with the decision variable. By introducing augmentation and proximal regularization terms to $\mathcal{L}(\mathbf{a}, \boldsymbol{\mu}, \boldsymbol{\nu})$ we obtain the augmented Lagrangian:

$$\tilde{\mathcal{L}}_{\rho,\gamma}(\mathbf{a}, \boldsymbol{\mu}, \boldsymbol{\nu}; \mathbf{a}') = \sum_{\mathbf{j}\in\mathcal{B}}\left[\mathcal{L}_{\mathbf{j}}(\mathbf{a_j}, \boldsymbol{\mu_j}, \boldsymbol{\nu}) + \frac{\rho\gamma_{\mathbf{j}}}{2}\left\|\tilde{\mathbf{G}}_{\mathbf{j}}\mathbf{a_j}\right\|_2^2\right] + \sum_{\mathbf{j}\in\mathcal{B}}\left[\frac{\rho\gamma_{\mathbf{j}}}{2}\left\|\mathbf{A}_{\mathbf{j},-}\mathbf{a}\right\|_2^2 + \frac{1}{2\rho}\left\|\mathbf{a_j} - \mathbf{a}'_{\mathbf{j}}\right\|_2^2\right] \tag{23}$$

Given that, $\tilde{\mathcal{L}}_{\mathbf{j}}(\mathbf{a_j}, \boldsymbol{\mu_j}, \boldsymbol{\nu}; \mathbf{a}'_{\mathbf{j}}) = \mathcal{L}_{\mathbf{j}}(\mathbf{a_j}, \boldsymbol{\mu_j}, \boldsymbol{\nu}) + \frac{1}{2\rho}\|\mathbf{a_j} - \mathbf{a}'_{\mathbf{j}}\|_2^2$ we can express it more compactly as:

$$\tilde{\mathcal{L}}_{\rho,\gamma}(\mathbf{a}, \boldsymbol{\mu}, \boldsymbol{\nu}; \mathbf{a}') \triangleq \sum_{\mathbf{j}\in\mathcal{B}}\left[\tilde{\mathcal{L}}_{\mathbf{j}}\left(\mathbf{a_j}, \boldsymbol{\mu_j}, \boldsymbol{\nu}; \mathbf{a}'_{\mathbf{j}}\right)\right] + \sum_{\mathbf{j}\in\mathcal{B}}\left[\frac{\rho\gamma_{\mathbf{j}}}{2}\left\|\tilde{\mathbf{G}}_{\mathbf{j}}\mathbf{a_j}\right\|_2^2 + \frac{\rho\gamma_{\mathbf{j}}}{2}\left\|\mathbf{A}_{\mathbf{j},-}\mathbf{a}\right\|_2^2\right] \tag{24}$$

where $\rho > 0$ is the *step-size* and $\gamma > 0$ is the over-relaxation term. The augmentation terms can be linearized around a prior primal iteration ($\mathbf{a}'_{\mathbf{j}}$ and $\mathbf{a}'$) as:

$$\frac{\rho\gamma_{\mathbf{j}}}{2}\left\|\tilde{\mathbf{G}}_{\mathbf{j}}\mathbf{a_j}\right\|_2^2 \approx \frac{\rho\gamma_{\mathbf{j}}}{2}\left\|\tilde{\mathbf{G}}_{\mathbf{j}}\mathbf{a}'_{\mathbf{j}}\right\|_2^2 + \rho\gamma_{\mathbf{j}}\left(\mathbf{a_j} - \mathbf{a}'_{\mathbf{j}}\right)^T\tilde{\mathbf{G}}_{\mathbf{j}}^T\tilde{\mathbf{G}}_{\mathbf{j}}\mathbf{a}'_{\mathbf{j}} \tag{25}$$

$$\frac{\rho\gamma_{\mathbf{j}}}{2}\left\|\mathbf{A}_{\mathbf{j},-}\mathbf{a}\right\|_2^2 \approx \frac{\rho\gamma_{\mathbf{j}}}{2}\left\|\mathbf{A}_{\mathbf{j},-}\mathbf{a}'\right\|_2^2 + \rho\gamma_{\mathbf{j}}\left(\mathbf{a_j} - \mathbf{a}'_{\mathbf{j}}\right)^T\mathbf{A}_{\mathbf{j},-}^T\mathbf{A}_{\mathbf{j},-}\mathbf{a}'_{\mathbf{j}} \tag{26}$$

Application of (25) and (26) to (24) yields:

$$\tilde{\mathcal{L}}_{\rho,\gamma}(\mathbf{a}, \boldsymbol{\mu}, \boldsymbol{\nu}; \mathbf{a}') = \sum_{\mathbf{j}\in\mathcal{B}}\left[\tilde{\mathcal{L}}_{\mathbf{j}}\left(\mathbf{a_j}, \boldsymbol{\mu_j}, \boldsymbol{\nu}; \mathbf{a}'_{\mathbf{j}}\right) + \left\langle\rho\gamma_{\mathbf{j}}\tilde{\mathbf{G}}_{\mathbf{j}}\mathbf{a}'_{\mathbf{j}}, \tilde{\mathbf{G}}_{\mathbf{j}}\mathbf{a_j}\right\rangle\right] + \sum_{\mathbf{j}\in\mathcal{B}}\left[\left\langle\rho\gamma_{\mathbf{j}}\mathbf{A}_{\mathbf{j},-}\mathbf{a}'_{\mathbf{j}}, \mathbf{A}_{\mathbf{j},-}\mathbf{a_j}\right\rangle\right]. \tag{27}$$

To maintain complete privacy of the algorithm, we use two atomic-specific over-relaxation terms: $\gamma_{\mathbf{j}}, \hat{\gamma}_{\mathbf{j}} > 0$ where $\gamma_{\mathbf{j}} > \hat{\gamma}_{\mathbf{j}}$. Thus, we can express the new 'predicted' dual updates in (27) as:

$$\tilde{\boldsymbol{\mu}}_{\mathbf{j}} = \boldsymbol{\mu}_{\mathbf{j}} + \rho\hat{\gamma}_{\mathbf{j}}\tilde{\mathbf{G}}_{\mathbf{j}}\mathbf{a}'_{\mathbf{j}}, \forall\mathbf{j} \in \mathcal{B}$$
$$\tilde{\boldsymbol{\nu}}_{\mathbf{j}} = \boldsymbol{\nu}_{\mathbf{j}} + \rho\hat{\gamma}_{\mathbf{j}}\mathbf{A}_{\mathbf{j},-}\mathbf{a}'_{\mathbf{j}}, \forall\mathbf{j} \in \mathcal{B}$$

Finally, we can write (27) as:

$$\tilde{\mathcal{L}}_{\rho,\gamma}(\mathbf{a}, \boldsymbol{\mu}, \boldsymbol{\nu}; \mathbf{a}') = \sum_{\mathbf{j}\in\mathcal{B}}\tilde{\mathcal{L}}_{\mathbf{j}}\left(\mathbf{a_j}, \tilde{\boldsymbol{\mu}}_{\mathbf{j}}, \tilde{\boldsymbol{\nu}}; \mathbf{a}'_{\mathbf{j}}\right). \tag{28}$$

APPENDIX B
CONVERGENCE OF PAC ALGORITHM

Before stating the main result regarding the convergence of the PAC algorithm, it is convenient to define the following auxiliary matrices:

$$\tilde{\mathbf{G}} = \mathbf{diag}\left\{\tilde{\mathbf{G}}_{\mathbf{1}}, \ldots, \tilde{\mathbf{G}}_{\mathbf{K}}\right\}$$
$$\boldsymbol{\Gamma}^{\tilde{\mathbf{G}}} = \mathbf{diag}\left\{\gamma_{\mathbf{1}}\mathbf{I}_{\mathbf{N}_1^{\mathbf{C}}}, \ldots, \gamma_{|\mathcal{B}|}\mathbf{I}_{\mathbf{N}_{|\mathcal{B}|}^{\mathbf{C}}}\right\}$$
$$\boldsymbol{\Gamma}^{\mathbf{A}} = \mathbf{diag}\left\{\gamma_{\mathbf{1}}\mathbf{I}_{\mathbf{N}_1^{\mathbf{O}}}, \ldots, \gamma_{|\mathcal{B}|}\mathbf{I}_{\mathbf{N}_{|\mathcal{B}|}^{\mathbf{O}}}\right\}$$
$$\mathbf{V_1} = \tilde{\mathbf{G}}^T\tilde{\mathbf{G}} + \mathbf{A}^T\mathbf{A}$$
$$\tilde{\mathbf{V}}_{\mathbf{1}}(\boldsymbol{\Gamma}) = \tilde{\mathbf{G}}^T\boldsymbol{\Gamma}^{\tilde{\mathbf{G}}}\tilde{\mathbf{G}} + \mathbf{A}^T\boldsymbol{\Gamma}^{\mathbf{A}}\mathbf{A}$$

Asymptotic convergence of the distributed PAC algorithm given by (10)-(15) is established through the following theorem.

Theorem 1 [6], [7]: Consider the ROPF formulation of (1) and its atomized variant (9). Let $\hat{F}_{\mathbf{j}}$ be a closed, convex and proper (CCP) function for all $\mathbf{j} \in \mathcal{B}$ and $\mathbf{a}[\tau]$, $\boldsymbol{\mu}[\tau]$, $\tilde{\boldsymbol{\mu}}[\tau]$, $\boldsymbol{\nu}[\tau]$, and $\tilde{\boldsymbol{\nu}}[\tau]$ be the primal and dual variable trajectories of (10)-(15) under zero initial conditions. Further, let $\mathbf{a}^*$ be the optimal primal solution to (9) and $\rho, \gamma_{\mathbf{j}}, \hat{\gamma}_{\mathbf{j}}$ the PAC parameters. For a matrix B, we let $\lambda_{\mathbf{min}}(B)$, $\hat{\lambda}_{\mathbf{min}}(B)$ and $\lambda_{\mathbf{max}}(B)$ represent the smallest, smallest non-zero, and largest eigenvalue, respectively of B. We further define $\gamma_{\mathbf{max}} \triangleq \max_{\mathbf{j}\in\mathcal{B}}\{\gamma_{\mathbf{j}}\}$, and $\gamma_{\mathbf{min}} \triangleq \min_{\mathbf{j}\in\mathcal{B}}\{\gamma_{\mathbf{j}}\}$.

Then, we have that:

a) If:

$$1 > \rho^2\gamma_{\mathbf{max}}\lambda_{\mathbf{max}}(\mathbf{V_1}) \tag{29}$$

then $\mathbf{lim}_{\tau\to\infty}\{\mathbf{a}[\tau]\} \to \mathbf{a}^*$ with rate $o(\frac{1}{\tau})$

b) If:

$$1 \geq \rho^2\gamma_{\mathbf{max}}\lambda_{\mathbf{max}}(\mathbf{V_1}) \tag{30}$$

then for the ergodic averaged trajectory $\bar{\mathbf{a}}[\tau] \triangleq \frac{1}{\tau}\sum_{s=0}^{\tau}\mathbf{a}[s]$, we have:

$$\left|\hat{F}(\bar{\mathbf{a}}[\tau]) - \hat{F}(\mathbf{a}^*)\right| \leq \left(\frac{1}{\tau}\right)\xi_{\mathbf{E1}}^{-1}(\rho, \gamma_{\mathbf{max}}) \tag{31}$$

$$\left\|\mathbf{R}^{\boldsymbol{\Gamma}}\bar{\mathbf{a}}[\tau]\right\|_2^2 \leq \left(\frac{1}{\tau}\right)\xi_{\mathbf{E2}}^{-1}(\rho, \gamma_{\mathbf{max}}) \tag{32}$$

where:

$$\mathbf{R}^{\boldsymbol{\Gamma}}\mathbf{R}^{\boldsymbol{\Gamma}} \tag{33}$$

and:

$$\xi_{\mathbf{E1}}(\rho, \gamma_{\mathbf{max}}) = \frac{\rho}{2}\left[\left\|\mathbf{a}^*\right\|_2^2 + \frac{4\Phi^2}{\gamma_{\mathbf{min}}\hat{\lambda}_{\mathbf{min}}(\mathbf{V_1})}\right]^{-1} \tag{34}$$

$$\xi_{\mathbf{E2}}(\rho, \gamma_{\mathbf{max}}) = \frac{\rho^2}{2}\left[\left\|\mathbf{a}^*\right\|_2^2 + 4\rho^2 + \frac{4\Phi^2}{\gamma_{\mathbf{min}}\hat{\lambda}_{\mathbf{min}}(\mathbf{V_1})}\right]^{-1} \tag{35}$$

where $\Phi = \mathbf{sup}_{\mathbf{z}\in\partial\hat{F}(\mathbf{a}^*)}\{\|\mathbf{z}\|_2\}$.

Intuitively, Theorem 1 guarantees that the nodal generation and consumption profiles obtained upon convergence of the PAC algorithm coincide with the optimal solution of the centralized OPF problem.

ACKNOWLEDGMENT

The authors would like to thank Dr. Anurag Srivastava and Dr. Anjan Bose of WSU, and Giulio Ferro and Yohan John of MIT for several useful discussions and comments. This material was prepared as an account of work (partially) sponsored by an agency of the United States Government.

[2]The *root* $\mathbf{R}$ exists since $\mathbf{V_1}$ is square p.s.d. matrix. Specifically, if $\mathbf{V_1} = \mathbf{U\Sigma U}^T$ is a suitable eigenvalue decomposition, then $\mathbf{R} = [\mathbf{U\Sigma}^{\frac{1}{2}}\mathbf{U}^T]$.

REFERENCES

[1] *ISO New England Pricing Reports*, ISO New England, Holyoke, MA, USA, 2018. [Online]. Available: https://www.iso-ne.com/isoexpress/web/reports/pricing/-/tree/ancillary

[2] P. Maloney. (Feb. 2018). *FERC Order Opens 'Floodgates' for Energy Storage in Wholesale Markets*. [Online]. Available: https://www.utilitydive.com/news/ferc-order-opens-floodgates-for-energy-storage-in-wholesale-markets/517326/

[3] F. C. Schweppe, M. C. Caramanis, R. D. Tabors, and R. E. Bohn, *Spot Pricing of Electricity*. New York, NY, USA: Springer, 1998.

[4] P. Huang *et al.*, "Analytics and transactive control design for the pacific northwest smart grid demonstration project," in *Proc. 1st IEEE Int. Conf. Smart Grid Commun.*, Gaithersburg, MD, USA, Oct. 2010, pp. 449–454.

[5] F. Rahimi and A. Ipakchi, "Using a transactive energy framework: Providing grid services from smart buildings," *IEEE Electrific. Mag.*, vol. 4, no. 4, pp. 23–29, Dec. 2016.

[6] J. Romvary, "A proximal atomic coordination algorithm for distributed optimization in distribution grids," Ph.D. dissertation, Dept. Elect. Eng. Comput. Sci., Massachusetts Inst. Technol., Cambridge, MA, USA, 2018.

[7] J. Romvary, G. Ferro, R. Haider, and A. Annaswamy, "A distributed proximal atomic coordination algorithm," *IEEE Trans. Autom. Control*, to be published.

[8] M. Yazdanian and A. Mehrizi-Sani, "Distributed control techniques in microgrids," *IEEE Trans. Smart Grid*, vol. 5, no. 6, pp. 2901–2909, Nov. 2014.

[9] K. E. Antoniadou-Plytaria, I. Kouveliotis-Lysikatos, P. S. Georgilakis, and N. D. Hatziargyriou, "Distributed and decentralized voltage control of smart distribution networks: Models, methods, and future research," *IEEE Trans. Smart Grid*, vol. 8, no. 6, pp. 2999–3008, Nov. 2017.

[10] T. Chen, Q. Alsafasfeh, H. Pourbabak, and W. Su, "The next-generation us retail electricity market with customers and prosumers—A bibliographical survey," *Energies*, vol. 11, no. 1, p. 8, 2018.

[11] S. D. Manshadi and M. E. Khodayar, "A hierarchical electricity market structure for the smart grid paradigm," *IEEE Trans. Smart Grid*, vol. 7, no. 4, pp. 1866–1875, Jul. 2016.

[12] M. Hofling, F. Heimgartner, B. Litfinski, and M. Menth, "A perspective on the future retail energy market," in *Proc. Int. Workshops SOCNET FGENET*, 2014, pp. 87–95.

[13] S. Parhizi, A. Khodaei, and S. Bahramirad, "Distribution market clearing and settlement," in *Proc. IEEE Power Energy Society Gen. Meeting*, Boston, MA, USA, Jul. 2016, pp. 1–5.

[14] L. Bai, J. Wang, C. Wang, C. Chen, and F. F. Li, "Distribution locational marginal pricing (DLMP) for congestion management and voltage support," *IEEE Trans. Power Syst.*, vol. 33, no. 4, pp. 4061–4073, Jul. 2018.

[15] Y. K. Renani, M. Ehsan, and M. Shahidehpour, "Optimal transactive market operations with distribution system operators," *IEEE Trans. Smart Grids*, vol. 9, no. 6, pp. 6692–6701, Nov. 2018.

[16] J. Wei, Y. Zhang, F. Sahriatzadeh, and A. K. Srivastava, "DLMP using three-phase current injection OPF with renewables and demand response," *IET Renew. Power Gener.*, vol. 13, no. 7, pp. 1160–1167, May 2019.

[17] J. Wei, L. Corson, and A. K. Srivastava, "Three-phase optimal power flow based distribution locational marginal pricing and associated price stability," in *Proc. IEEE Power Energy Soc. Gen. Meeting*, Denver, CO, USA, Jul. 2015, pp. 1–5.

[18] C.-H. Lo and N. Ansari, "Decentralized controls and communications for autonomous distribution networks in smart grid," *IEEE Trans. Smart Grid*, vol. 4, no. 1, pp. 66–77, Mar. 2013.

[19] Z. Wang, B. Chen, J. Wang, and J. Kim, "Decentralized energy management system for networked microgrids in grid-connected and Islanded modes," *IEEE Trans. Smart Grid*, vol. 7, no. 2, pp. 1097–1105, Mar. 2016.

[20] N. Li, "A market mechanism for electric distribution networks," in *Proc. 54th Conf. Decis. Control (CDC)*, Osaka, Japan, Dec. 2015, pp. 2276–2282.

[21] T. Morstyn, A. Teytelboym, and M. D. McCulloch, "Designing decentralized markets for distribution system flexibility," *IEEE Trans. Power Syst.*, vol. 34, no. 3, pp. 2128–2139, May 2019.

[22] C. Pop, T. Cioara, M. Antal, I. Anghel, I. Salomie, and M. Bertoncini, "Blockchain based decentralized management of demand response programs in smart energy grids," *Sensors*, vol. 18, no. 1, p. 162, 2018.

[23] N. Zhang, Y. Yan, and S. Xu, "Game-theory-based electricity market clearing mechanisms for an open and transactive distribution grid," in *Proc. IEEE Power Energy Soc. Gen. Meeting*, Denver, CO, USA, Jul. 2015, pp. 1–5.

[24] M. Caramanis, E. Ntakou, W. W. Hogan, A. Chakrabortty, and J. Schoene, "Co-optimization of power and reserves in dynamic T and D power markets with nondispatchable renewable generation and distributed energy resources," *Proc. IEEE*, vol. 104, no. 4, pp. 807–836, Apr. 2016.

[25] K. F. Hong Zhou, Z.-W. Liu, and D. Hu, "Retail market pricing design in smart distribution networks considering wholesale market price uncertainty," in *Proc. IEEE 43rd Annu. Conf. Ind. Electron. Soc. (IECON 2017)*, Beijing, China, Nov. 2017, pp. 5968–5973.

[26] H. Pourbabak, T. Chen, and W. Su, "Consensus-based distributed control for economic operation of distribution grid with multiple consumers and prosumers," in *Proc. IEEE Power Energy Soc. Gen. Meeting (PESGM)*, Boston, MA, USA, Jul. 2016, pp. 1–5.

[27] N. Rahbari-Asr, U. Ojha, Z. Zhang, and M.-Y. Chow, "Incremental welfare consensus algorithm for cooperative distributed generation/demand response in smart grid," *IEEE Trans. Smart Grid*, vol. 5, no. 6, pp. 2836–2845, Nov. 2014.

[28] S. Kar, G. Hug, J. Mohammadi, and J. M. F. Moura, "Distributed state estimation and energy management in smart grids: A consensus+ innovations approach," *IEEE J. Sel. Topics Signal Process.*, vol. 8, no. 6, pp. 1022–1038, Dec. 2014.

[29] W. Shi, X. Xie, C.-C. Chu, and R. Gadh, "Distributed optimal energy management in microgrids," *IEEE Trans. Smart Grid*, vol. 6, no. 3, pp. 1137–1146, May 2015.

[30] Y. Zhang, N. Gatsis, and G. B. Giannakis, "Robust energy management for microgrids with high-penetration renewables," *IEEE Trans. Sustain. Energy*, vol. 4, no. 4, pp. 944–953, Oct. 2013.

[31] H. S. V. S. K. Nunna and S. Doolla, "Multiagent-based distributed-energy-resource management for intelligent microgrids," *IEEE Trans. Ind. Electron.*, vol. 60, no. 4, pp. 1678–1687, Apr. 2013.

[32] Y. Xu and Z. Li, "Distributed optimal resource management based on the consensus algorithm in a microgrid," *IEEE Trans. Ind. Electron.*, vol. 62, no. 4, pp. 2584–2592, Apr. 2015.

[33] Q. Sun, R. Han, H. Zhang, J. Zhou, and J. M. Guerrero, "A multiagent-based consensus algorithm for distributed coordinated control of distributed generators in the energy Internet," *IEEE Trans. Smart Grid*, vol. 6, no. 6, pp. 3006–3019, Nov. 2015.

[34] J. W. Simpson-Porco, Q. Shafiee, F. Dörfler, J. C. Vasquez, J. M. Guerrero, and F. Bullo, "Secondary frequency and voltage control of islanded microgrids via distributed averaging," *IEEE Trans. Ind. Electron.*, vol. 62, no. 11, pp. 7025–7038, Nov. 2015.

[35] L. Gan, N. Li, U. Topcu, and S. H. Low, "Exact convex relaxation of optimal power flow in radial networks," *IEEE Trans. Autom. Control*, vol. 60, no. 1, pp. 72–87, Jan. 2015.

[36] G. Chen and M. Teboulle, "A proximal-based decomposition method for convex minimization problems," *Math. Program.*, vol. 64, pp. 81–101, 1994. [Online]. Available: https://doi.org/10.1007/BF01582566

[37] N. Parikh and S. Boyd, "Proximal algorithms," *Found. Trends Optim.*, vol. 1, no. 3, pp. 123–231, 2013.

[38] A. Makhdoumi and A. Ozdaglar, "Convergence rate of distributed ADMM over networks," *IEEE Trans. Autom. Control*, vol. 52, no. 10, pp. 5082–5095, Oct. 2017.

[39] Y. Hayashi *et al.*, "Versatile modeling platform for cooperative energy management systems in smart cities," *Proc. IEEE*, vol. 106, no. 4, pp. 594–612, Apr. 2018.

[40] "Standard models for Japanese power system, (in Japanese)" IEEJ, Tokyo, Japan, IEEJ Rep. 754, 1999.
[41] *TEP Company*. Accessed: May 15, 2019. [Online]. Available: https://www4.tepco.co.jp/en/forecast/html/index-e.html
[42] *JEP eXchange*. Accessed: May 15, 2019. [Online]. Available: http://www.jepx.org/english/index.html
[43] *Average Electricity Prices Around the World: $/kwh*, OVO Energy, Bristol, U.K., 2019. [Online]. Available: https://www.ovoenergy.com/guides/energy-guides/average-electricity-prices-kwh.html
[44] *Electricity Rate Plans*, TEP Company, Ginza, Tokyo, 2019. [Online]. Available: https://www7.tepco.co.jp/ep/rates/electricbill-e.html
[45] "IEEE PES AMPS DSAS test feeder working group: Resources," Dept. E Soc., IPower, Burlington, MA, USA, Rep., 1992.
[46] *Energy, Load, and Demand Reports*, ISO-NE, Holyoke, MA, USA, 2019. [Online]. Available: https://www.iso-ne.com/isoexpress/web/reports/load-and-demand/-/tree/dmnd-five-minute-sys
[47] *Pricing Reports*, ISO-NE, Holyoke, MA, USA, 2019. [Online]. Available: https://www.iso-ne.com/isoexpress/web/reports/pricing/-/tree/lmps-rt-five-minute-final
[48] Y. Zhang, M. Hong, E. Dall'Anese, S. Dhople, and Z. Xu, "Distributed controllers seeking AC optimal power flow solutions using ADMM," *IEEE Trans. Smart Grid*, vol. 9, no. 5, pp. 4525–4537, Sep. 2018.
[49] P. Kansal and A. Bose, "Bandwidth and latency requirements for smart transmission grid applications," *IEEE Trans. Smart Grid*, vol. 3, no. 3, pp. 1344–1352, Sep. 2012.
[50] Y.-J. Kim, M. Thottan, V. Kolesnikov, and W. Lee, "A secure decentralized data-centric information infrastructure for smart grid," *IEEE Commun. Mag.*, vol. 48, no. 11, pp. 58–65, Nov. 2010.
[51] M. Kuzlu, M. Pipattanasomporn, and S. Rahman, "Communication network requirements for major smart grid applications in HAN, NAN, and WAN," *Comput. Netw.*, vol. 67, pp. 74–88, Jul. 2014.